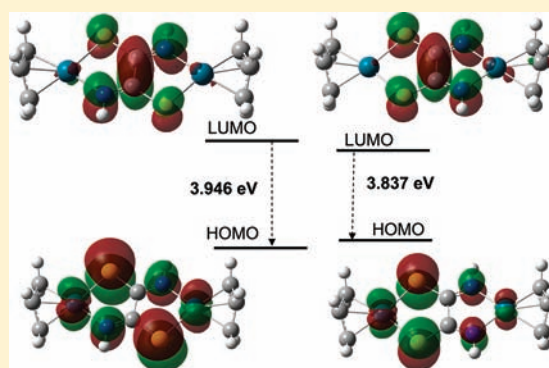


Allylpalladium Dimers with Metals Connected by Binucleating Dithiooxamidates in Two Different Coordination Modes: Solution Behavior and Solid-State Structure

Santo Lanza,^{*,†} Francesco Nicolò,[†] Hadi Amiri Rudbari,[†] Maria Rosaria Plutino,[‡] and Giuseppe Bruno[†]

[†]Dipartimento di Chimica Inorganica, Chimica Analitica e Chimica Fisica, and [‡]Istituto per lo Studio dei Materiali Nanostrutturati (ISMN-CNR, OU Palermo, unità di Messina), c/o Dipartimento di Chimica Inorganica, Chimica Analitica e Chimica Fisica, Università di Messina, Salita Sperone, 31 Contrada Papardo, 98166 Messina, Italy

ABSTRACT: A series of allylpalladium dimers having metals connected by binucleating dialkyldithiooxamidate $[N(R)SC-CS(R)N]^{2-}$ [$R =$ methyl, ethyl, isopropyl, benzyl, isoamyl, (*S*)-1-(1-phenyl)ethyl, *meso*-(1-phenyl)ethyl, and *rac*-(1-phenyl)ethyl] were prepared by reacting the monochelate $[(\eta^3\text{-allyl})Pd(N(R)SC-CS(R)NH \kappa\text{-S,S} Pd)]$ with $[(\eta^3\text{-allyl})PdCl]_2$ in chloroform. At low temperature (20 °C), the bimetallic complexes $[(\eta^3\text{-allyl})Pd]_2(\mu\text{-dialkyldithiooxamidate } \kappa\text{-N,N}' Pd, \kappa\text{-S,S}' Pd')$ (kinetic compounds) are formed in a short reaction time (10 min). At a higher temperature (50 °C) and a longer reaction time (24 h), the corresponding bimetallic isomers $[(\eta^3\text{-allyl})Pd]_2(\mu\text{-dialkyldithiooxamidate } \kappa\text{-N,S} Pd, \kappa\text{-N}',S' Pd')$ (thermodynamic compounds) are obtained. Both kinetic and thermodynamic compounds can exist as endo or exo isomers, depending on the reciprocal orientation of the allyl



cusps. Both endo and exo isomers are only detectable in solution when the alkyl substituents are chiral alkyl groups. Moreover, diffractometric modeling agrees with the presence of both isomers in the solid state even when the alkyl substituent is an achiral alkyl group. In a chloroform solution, endo and exo isomers undergo isomeric conversion owing to the apparent allyl rotation that follows the Pd–N bond rupture in the $(\eta^3\text{-allyl})Pd(N^{\wedge}N)$ frame of kinetic compounds or in the $(\eta^3\text{-allyl})Pd(N^{\wedge}S)$ frame of thermodynamic compounds. The dithiooxamidate $[N(R)SC-CS(R)N]^{2-}$, when engaged in a $\kappa\text{-N,S} Pd, \kappa\text{-N}',S' Pd'$ coordination mode, behaves as a hybrid hemilabile binucleating ligand. At room temperature and in a chloroform solution, the kinetic compounds rearrange into the thermodynamically more stable isomers in about 3 or 4 days. The higher stability of the thermodynamic species was evaluated by means of computational studies in accordance with the maximum hardness principle. Finally, the crystal structures of $[(\eta^3\text{-allyl})Pd]_2(\mu\text{-diethylthiooxamidate } \kappa\text{-N,S} Pd, \kappa\text{-N}',S' Pd')$, $[(\eta^3\text{-allyl})Pd]_2(\mu\text{-meso-(1-phenyl)ethylthiooxamidate } \kappa\text{-N,S} Pd, \kappa\text{-N}',S' Pd')$, and $[(\eta^3\text{-allyl})Pd]_2(\mu\text{-rac-(1-phenyl)ethylthiooxamidate } \kappa\text{-N,N}' Pd, \kappa\text{-S,S}' Pd')$ are reported.

INTRODUCTION

Secondary dithiooxamides (DTOs), $HN(R)SC-CS(R)NH$ (hereafter referred to as H_2R_2DTO), can behave as ditopic ligands, which can bind two metal fragments in a variety of coordination modes because of their different donor sites and their freely rotating $N(R)CS$ moieties.

The $\kappa\text{-N,S} ML_n, \kappa\text{-N}',S' M'L'n$ and $\kappa\text{-S,S}' ML_n, \kappa\text{-N,N}' M'L'n$ modes (A and B in Chart 1) have been extensively investigated.^{1–6} However, even the less common “exo” $\kappa\text{-N,S} ML_n$ mode (C in Chart 1) has been suggested⁷ and recently well documented.⁸

The different ways in which two metal fragments can be connected depends on a delicate balance of the following steric and electronic factors: (i) the nature of the alkyl substituents of amidic nitrogen atoms in the ligand; (ii) the hard–soft character of both coordinated metals and ligand donor sites; (iii) the nature of the ancillary ligands in the binucleated metal fragments. Accordingly, it has been observed that DTO, if reacted with some chloro-bridged dimers, forms homobimetallic complexes in a

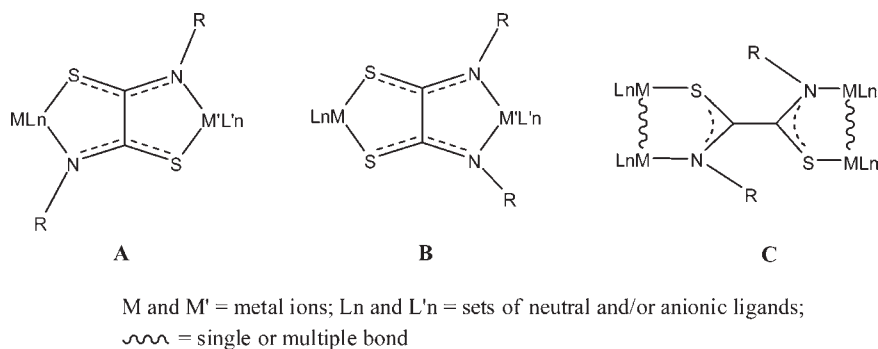
$\kappa\text{-N,S}$ binucleation mode if the amidic nitrogen atoms bear secondary carbon atoms ($-CH_2R$) as substituents.⁹ Furthermore, it has been demonstrated that the hardness or softness of the metal fragments in a heterobimetallic complex produces specific interactions with the sulfur or nitrogen chelating system of the binucleating DTO.¹⁰ Moreover, it has been observed that the steric hindrance of the ancillary ligands in a given metal fragment can also favor the formation of one of the two possible linkage isomers of the $\kappa\text{-N,N}' ML_n \kappa\text{-S,S}' M'L'n$ bimetallic complexes.¹¹ Finally, it has been shown that the bulkiness of nitrogen DTO substituents can direct the synthesis of homobimetallic complexes in an “exo” $\kappa\text{-N,S}$ coordination mode toward one of the two possible conformers.⁸

The present paper explores the capability of a secondary DTO to act as a binucleating ligand when the ancillary ligands in the binucleated metal frames have modest steric crowding. The aim

Received: July 27, 2011

Published: October 18, 2011

Chart 1. Coordination Modes of Dialkyldithiooxamidate as a Binucleating Ligand



is to achieve full control of the stereochemistry of the poly-metallic systems built by means of multifunctional binucleating ligands.

EXPERIMENTAL PART

All chemicals were standard reagent grade and were used without further purification. Column chromatography was conducted on alumina oxide (activated, neutral, Brockman grade I).

^1H and ^{13}C NMR spectra were recorded at room temperature in CDCl_3 , on a Bruker ARX 300 spectrometer at 300 and 75 MHz, respectively, and on a VNMR5 Varian Instruments spectrometer at 500 MHz, using the residual proton resonance of the solvent as the δ reference.

$[(\eta^3\text{-Allyl})\text{Pd}(\text{HR}_2\text{-DTO } \kappa\text{-S,S } \text{Pd})]$ was prepared following a reported procedure.¹¹ Secondary DTOs, $\text{H}_2\text{R}_2\text{DTO}$ [R = methyl, ethyl, isopropyl, benzyl, isoamyl, 1-(S)-(1-phenyl)ethyl, and *meso/rac*-(1-phenyl)ethyl], were prepared according to literature methods.¹² The *meso*-DTO H-(R)-(1-(1-phenyl)ethyl)NSC-CSN-(S)-(1-(1-phenyl)ethyl)-H was obtained by fractional crystallization from ethanol and an equimolar mixture of *meso*- and *rac*-(1-phenyl)ethyldithiooxamide obtained from *rac*-(1-phenyl)ethylamine. $[(\eta^3\text{-Allyl})\text{PdCl}]_2$ is a commercial product (Aldrich).

X-ray structure determination of $[(\eta^3\text{-allyl})\text{Pd}]_2(\mu\text{-diisoamyl-DTO } \kappa\text{-N,S } \text{Pd}, \kappa\text{-N',S' } \text{Pd}')$, $[(\eta^3\text{-allyl})\text{Pd}]_2(\mu\text{-meso-(1-phenyl)ethyl-DTO } \kappa\text{-N,S } \text{Pd}, \kappa\text{-N',S' } \text{Pd}')$ (*meso*-(1-phenyl)ethyl-DTO = [(R)-1-(1-phenyl)ethyl]-NSC-CSN-(S)-(1-(1-phenyl)ethyl)]²⁻) and $[(\eta^3\text{-allyl})\text{Pd}]_2(\mu\text{-rac-(1-phenyl)ethyl-DTO } \kappa\text{-N,N' } \text{Pd}, \kappa\text{-S,S' } \text{Pd}')$ (*rac*-(1-phenyl)ethyl-DTO = [(1-(R)-(1-phenyl)ethyl)-NSC-CSN-(1-(R)-(1-phenyl)ethyl)]²⁻ / [(1-(S)-(1-phenyl)ethyl)-NSC-CSN-(1-(S)-(1-phenyl)ethyl)]²⁻) (50:50) was done.

Yellow/orange crystals of suitable quality for X-ray analysis were selected from those crystallized from a chloroform/petroleum ether solution of each of the above three complexes.

Data were collected at room temperature with a Bruker APEX II CCD area-detector diffractometer using Mo $K\alpha$ radiation ($\lambda = 0.71073 \text{ \AA}$). Data collection, cell refinement, data reduction, and absorption correction were performed using multiscan methods with Bruker software.¹³ The structures were solved by direct methods using *SIR2004*.¹⁴

The non-hydrogen atoms were refined anisotropically by the full-matrix least-squares method on F^2 using *SHELXL*.¹⁵ All of the hydrogen atoms were placed at calculated positions and constrained to ride on their parent atoms. Molecular structures are shown in Figures 6–8.

Computational Study. All calculations were performed with the *Gaussian 03* suite of programs.¹⁶ Geometry optimizations and harmonic frequencies for the complexes were calculated with density functional theory using the PBE1PBE functional with different basis sets for the idealized C_2 and C_s symmetries. The geometries were restricted to the

highest reasonable symmetry, and each stationary point was confirmed to be a minimum on the potential energy surface by yielding zero imaginary vibrational frequencies in the vibrational frequency analysis. The geometries were constructed by *GaussView 3.09*, available from Gaussian Inc. (Pittsburgh, PA),¹⁶ which was also used to produce pictures of the orbitals. The best agreement with X-ray crystal structure data was achieved using the PBE1PBE^{17,18} functional in conjunction with the large 6-311++G(2df,2p) and full-relativistic effective core potential aug-cc-pVTZ-PP¹⁹ basis set used for carbon, nitrogen, hydrogen, sulfur, and palladium.

General procedures for the preparation of homobinuclear complexes $[(\eta^3\text{-allyl})\text{Pd}]_2(\mu\text{-R}_a\text{R}_b\text{-DTO } \kappa\text{-N,S } \text{Pd}, \kappa\text{-N',S' } \text{Pd}')$ [$\text{R}_a = \text{R}_b = \text{methyl}$, 1; $\text{R}_a = \text{R}_b = \text{ethyl}$, 2; $\text{R}_a = \text{R}_b = \text{isopropyl}$, 3; $\text{R}_a = \text{R}_b = \text{benzyl}$, 4; $\text{R}_a = \text{R}_b = \text{isoamyl}$, 5; $\text{R}_a = \text{R}_b = 1\text{-(S)-(1-phenyl)ethyl}$, 6; $\text{R}_a = 1\text{-(S)-(1-phenyl)ethyl}$; $\text{R}_b = 1\text{-(R)-(1-phenyl)ethyl}$, 7]:

A total of 1 mmol (365 mg) of $[(\eta^3\text{-allyl})\text{PdCl}]_2$ was dissolved in chloroform (100 mL) and then reacted with 2 mol equiv of the selected $\text{H}_2\text{R}_2\text{DTO}$ species. The solution turned orange and was left to stand for $1/2$ h at room temperature. After the addition under stirring of 2 g of sodium bicarbonate, the solution turned bright yellow. After filtration of bicarbonate, the yellow filtrate, which contained $[(\eta^3\text{-allyl})\text{Pd}(\text{H-R}_2\text{-DTO } \kappa\text{-S,S } \text{Pd})]$, was reacted with 1 mmol (365 mg) of $[(\eta^3\text{-allyl})\text{PdCl}]_2$. The mixture was refluxed for 24 h at 50 °C, the solvent was removed, and the crude product was redissolved in a minimum amount of chloroform and loaded on an alumina column equilibrated with petroleum ether. Elution with a petroleum ether/chloroform mixture (90:10) gave a yellow fraction from which the homobimetallic $[(\eta^3\text{-allyl})\text{Pd}]_2(\mu\text{-R}_2\text{-DTO } \kappa\text{-N,S } \text{Pd}, \kappa\text{-N',S' } \text{Pd}')$ was crystallized.

$[(\eta^3\text{-Allyl})\text{Pd}]_2[\mu\text{-(methyl)}_2\text{-DTO } \kappa\text{-N,S } \text{Pd}, \kappa\text{-N',S' } \text{Pd}']$ (1). Yield: 0.37 g (41.7%). ^1H NMR (300 MHz, CDCl_3): δ 5.46 (m, 2H, allyl CH_2 CH CH_2), 4.03 and 3.57 (2d, 4H, allyl $\text{CHH}_{\text{syn}}\text{CHCHH}_{\text{syn}}$, $J_{\text{syn}} = 7.2$ Hz), 3.79 (s, 6H, NCH_3), 3.41 and 2.64 (2d, 4H, allyl $\text{CHH}_{\text{anti}}\text{CHCHH}_{\text{anti}}$, $J_{\text{anti}} = 12.6$ Hz). ^{13}C NMR (75 MHz, CDCl_3): δ 115.00 (allyl CH_2 CH CH_2), 69.54 and 58.20 (allyl CH_2 CH CH_2), 50.7 (NCH_3). Anal. Calcd for $\text{C}_{10}\text{H}_{16}\text{N}_2\text{S}_2\text{Pd}_2$: C, 27.22; H, 3.66; N, 6.35. Found: C, 27.41; H, 3.74; N, 6.49.

$[(\eta^3\text{-Allyl})\text{Pd}]_2[\mu\text{-(ethyl)}_2\text{-DTO } \kappa\text{-N',S' } \text{Pd } \kappa\text{-N,S } \text{Pd}']$ (2). Yield: 0.43 g (45.6%). ^1H NMR (300 MHz, CDCl_3): δ 5.44 (2 m, 2H, allyl CH_2 CH CH_2), 4.17 (m, 4H, NCH_2CH_3), 4.00 and 3.55 (2d, 4H, allyl $\text{CHH}_{\text{syn}}\text{CHCHH}_{\text{syn}}$, $J_{\text{syn}} = 7.2$ Hz), 3.36 and 2.63 (2d, 4H, allyl $\text{CHH}_{\text{anti}}\text{CHCHH}_{\text{anti}}$, $J_{\text{anti}} = 14.2$ Hz), 1.29 (t, 6H, NCH_2CH_3 , $^3J_{\text{H-H}} = 6.8$ Hz). ^{13}C NMR (75 MHz, CDCl_3): δ 114.5 (allyl CH_2 CH CH_2), 68.6 and 56.24 (allyl CH_2 CH CH_2), 49.78 (NCH_2CH_3), 20.50 (NCH_2CH_3). Anal. Calcd for $\text{C}_{12}\text{H}_{20}\text{N}_2\text{S}_2\text{Pd}_2$: C, 30.71; H, 4.30; N, 5.97. Found: C, 30.68; H, 4.36; N, 6.08.

$[(\eta^3\text{-Allyl})\text{Pd}]_2[\mu\text{-(isopropyl)}_2\text{-DTO } \kappa\text{-N,S } \text{Pd}, \kappa\text{-N',S' } \text{Pd}']$ (3). Yield: 0.40 g (40.0%). ^1H NMR (300 MHz, CDCl_3): δ 5.32

(m, 2H, allyl CH₂CHCH₂), 4.94 (sl, 2H, NCH(CH₃), ³J_{H-H} = 6.3 Hz), 4.42 and 4.16 (2d, 4H, allyl CHH_{syn}CHCHH_{syn}, J_{syn} = 6.6 Hz), 2.94 and 2.91 (2d, 4H, allyl CHH_{anti}CHCHH_{anti}, J_{anti} = 12.2 Hz), 1.20 and 1.10 (2d, 12H, NCH(CH₃), ³J_{H-H} = 6.3 Hz). ¹³C NMR (75 MHz, CDCl₃): δ 112.36 (allyl CH₂CHCH₂), 67.81 and 57.43 (allyl CH₂CHCH₂), 50.60 (NCH(CH₃)₂), 22.26 and 21.71 (NCH(CH₃)₂). Anal. Calcd for C₁₄H₂₄N₂S₂Pd₂: C, 33.81; H, 4.86; N, 5.63. Found: C, 33.92; H, 4.93; N, 5.70.

[(η³-Allyl)Pd]₂[μ-(benzyl)₂-DTO κ-N,S Pd, κ-N',S' Pd'] (4). Yield: 0.46 g (38.6%). ¹H NMR (300 MHz, CDCl₃): δ 7.38–7.21 (10H, NCH₂C₆H₆), 5.46 (AB spin system, 4H, NCH₂C₆H₆, ²J_{H-H} = 14.2 Hz), 5.17 (m, 2H, allyl CH₂CHCH₂), 5.73 and 3.52 (2d, 4H, CHH_{syn}CHCHH_{syn}, J_{syn} = 7.97 Hz), 2.85 and 2.53 (2d, 4H, CHH_{anti}CHCHH_{anti}, J_{anti} = 12.82 Hz). ¹³C NMR (75 MHz, CDCl₃): δ 138.0, 128.4, 127.7, 127.4, 126.9 (NCH₂C₆H₅), 114.17 (allyl CH₂CHCH₂), 69.15 and 67.12 (allyl CH₂CHCH₂), 64.24 (–NCH₂–). Anal. Calcd for C₂₂H₂₄N₂S₂Pd₂: C, 44.53; H, 4.08; N, 4.72. Found: C, 44.61; H, 4.18; N, 4.76.

[(η³-Allyl)Pd]₂[μ-(isoamyl)₂-DTO κ-N,S Pd, κ-N',S' Pd'] (5). Yield: 0.49 g (44.1%). ¹H NMR (300 MHz, CDCl₃): δ 5.54 (m, 2H, allyl CH₂CHCH₂), 4.13 (m, AB₂ spin system, 4H, NCH₂CH₂CH(CH₃)₂, 3.92 and 3.55 (2d, 4H, allyl CHH_{syn}CHCHH_{syn}, J_{syn} = 7.7 Hz), 3.34 and 2.61 (2d, 4H, CHH_{anti}CHCHH_{anti}, J_{anti} = 12.6 Hz), 1.72 and 1.64 (2m, 6H, NCH₂CH₂CH(CH₃)₂, 0.99 (d, 12H, NCH₂CH₂CH(CH₃)₂, ³J_{H-H} = 6.6 Hz). ¹³C{¹H} NMR (75 MHz, CDCl₃): δ 114.44 (allyl CH₂CHCH₂), 68.70 and 49.67 (allyl CH₂CHCH₂), 60.52 (NCH₂CH₂CH(CH₃)₂), 36.47 (NCH₂CH₂CH(CH₃)₂), 26.80 (NCH₂CH₂CH(CH₃)₂), 22.86 and 22.79 (NCH₂CH₂CH(CH₃)₂). Anal. Calcd for C₁₆H₂₈N₂S₂Pd₂: C, 36.58; H, 5.37; N, 5.33. Found: C, 36.69; H, 5.32; N, 5.24.

[(η³-allyl)Pd]₂[μ-((S)-1-(1-phenyl)ethyl)₂-DTO κ-N,S Pd, κ-N',S' Pd'] (6): Yield: 0.28 gr (22.4%). ¹H NMR (300 MHz, CDCl₃), δ (ppm): 7.44–7.22 (10H, N–CH(CH₃)–C₆H₆), 6.18 (m, 2H, N–CH(CH₃)–C₆H₆), 5.14, 5.13, 4.74, and 4.72 (4m, 2H, Allyl CH₂CHCH₂), 3.67, 3.67, 3.49, 3.48, 3.46, 3.45, 3.05, and 3.05 ppm (8d, 4H, Allyl CHH_{syn}CH–CHH_{syn}, J_{syn} = 7.1 Hz), 2.87, 2.87, 2.47, 2.47, 2.41, 2.40, 1.83, and 1.82 ppm (8d, 4H, Allyl CHH_{anti}CH–CHH_{anti}, J_{anti} = 12.6 Hz). 1.71, 1.69, 1.63, and 1.61 ppm (4d, 6H, N–CH(CH₃)–C₆H₆, ³J_{H-H} = 6.6 Hz). ¹³C NMR (75 MHz, CDCl₃), δ (ppm): 163.60, 143.30, 128.10, 128.00, 126.80, 126.70, 126.60 (N–CH(CH₃)–C₆H₅), 112.70, 112.10 (Allyl CH₂CH–CH₂), 68.40, 68.26, 62.30 (Allyl CH₂–CHCH₂), 50.90, 50.30 (N–CH(CH₃)–C₆H₅), 18.00, 17.60 (N–CH(CH₃)–C₆H₅). Anal. Calcd for C₂₄H₂₈N₂S₂Pd₂: C 46.38, H 4.54, N 4.51; Found: C 46.19, H 4.44, N 4.39.

[(η³-allyl)Pd]₂[μ-(meso-(1-phenyl)ethyl)-DTO κ-N,S Pd, κ-N',S' Pd'] (7): Yield: 0.25 gr (20.0%). ¹H NMR and ¹³C NMR, spectra identical to those of 6

Anal. Calcd for C₂₄H₂₈N₂S₂Pd₂: C 46.38, H 4.54, N 4.51; Found: C 46.30, H 4.35, N 4.39.

General procedures for the preparation of homobinuclear complexes [(η³-allyl)Pd]₂[μ-R_aR_b-DTO κ-N,N' Pd, κ-S,S' Pd'] (R_a=R_b = Methyl, 8; R_a=R_b = Ethyl, 9; R_a=R_b = Isopropyl, 10; R_a=R_b = Benzyl, 11; R_a=R_b = isoamyl, 12; R_a=R_b = 1-(S)-(1-phenyl)ethyl, 13; R_a=1-(S)-(1-phenyl)ethyl, R_b=1-(R)-(1-phenyl)ethyl, 14.; R_a=R_b = (1-(S)-1-phenyl)ethyl/(1-(R)-1-phenyl)ethyl (50:50); 15:

[(η³-allyl)PdCl]₂ (1 mmol, 365 mg) was dissolved in chloroform (100 mL) and two molar equivalents of the desired H₂R₂DTO species. The solution turned orange and was left to stand at room temperature for 1/2 h. On addition, under stirring, of 2 g of sodium bicarbonate, the solution turned bright yellow. After filtration of the bicarbonate, the yellow filtrate, which contained [(η³-allyl)Pd(H-R₂-DTO κ-S,S Pd)], was reacted with [(η³-allyl)PdCl]₂ (1 mmol, 365 mg) at room temperature for 1/2 h. The solvent was then removed and the crude product was redissolved in the minimum amount of chloroform and loaded on an

alumina column equilibrated with petroleum ether. Two yellow fractions were collected. The first one of lighter color was discarded while the other was collected which, upon crystallization, gave [(η³-allyl)Pd]₂(μ-R_aR_b-DTO κ-N,N' Pd, κ-S,S' Pd') complexes as yellow microcrystals.

[(η³-Allyl)Pd]₂[μ-(methyl)₂-DTO κ-N,N' Pd, κ-S,S' Pd'] (8). Yield: 0.41 g (46.2%). ¹H NMR (300 MHz, CDCl₃): δ 5.55 and 5.29 (2m, 2H, allyl CH₂CHCH₂), 4.02 and 3.57 (2d, 4H, allyl CHH_{syn}CHCHH_{syn}, J_{syn} = 7.2 Hz), 3.60 (s, 6H, NCH₃), 3.00 and 2.95 (2d, 4H, CHH_{anti}CHCHH_{anti}, J_{anti} = 12.6 Hz). ¹³C NMR (75 MHz, CDCl₃): δ 116.5 and 113.3 (allyl CH₂CHCH₂), 71.15 and 58.2 (allyl CH₂CHCH₂), 48.00 (NCH₃). Anal. Calcd for C₁₀H₁₆N₂S₂Pd₂: C, 27.22; H, 3.66; N, 6.35. Found: C, 27.53; H, 3.58; N, 6.42.

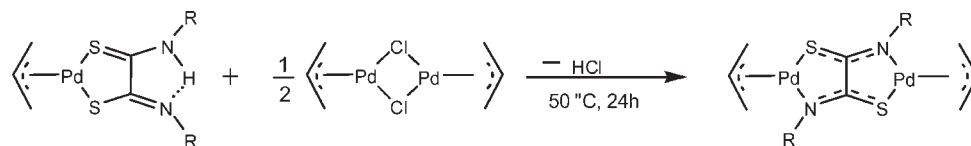
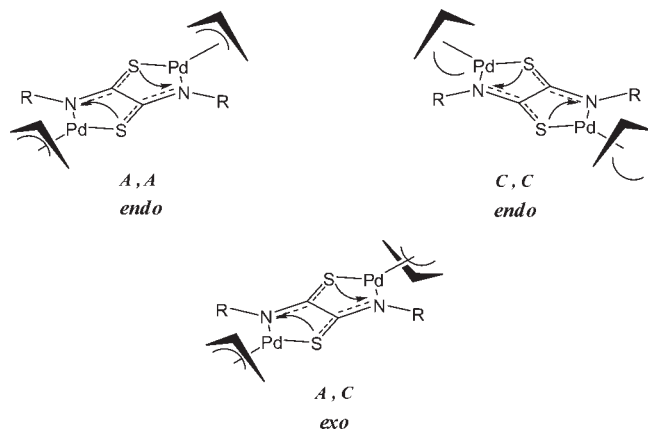
[(η³-Allyl)Pd]₂[μ-(ethyl)₂-DTO κ-N,N' Pd, κ-S,S' Pd'] (9). Yield: 0.38 g (40.3%). ¹H NMR (300 MHz, CDCl₃): δ 5.50 and 5.29 (2m, 2H, allyl CH₂CHCH₂), 4.00 and 3.60 (2d, 4H, CHH_{syn}CHCHH_{syn}, J_{syn} = 7.2 Hz), 3.98 (m, 4H, NCH₂CH₃), 2.99 and 2.93 (2d, 4H, CHH_{anti}CHCHH_{anti}, J_{anti} = 14.2 Hz), 1.26 (t, 6H, NCH₂CH₃, ³J_{H-H} = 6.8 Hz). ¹³C NMR (75 MHz, CDCl₃): δ 115.45 and 113.21 (allyl CH₂CHCH₂), 61.06 and 57.48 (allyl CH₂CHCH₂), 53.90 (NCH₂–), 13.89 (NCH₂CH₃). Anal. Calcd for C₁₂H₂₀N₂S₂Pd₂: C, 30.71; H, 4.30; N, 5.97. Found: C, 30.86; H, 4.32; N, 6.02.

[(η³-Allyl)Pd]₂[μ-(isopropyl)₂-DTO κ-N,N' Pd, κ-S,S' Pd'] (10). Yield: 0.33 g (29.7%). ¹H NMR (300 MHz, CDCl₃): δ 5.32 and 5.29 (2d, 2H, allyl CH₂CHCH₂), 4.91 (sl, 2H, NCH(CH₃)₂, ³J_{H-H} = 6.3 Hz), 4.15 and 3.97 (2m, 4H, CHH_{syn}CHCHH_{syn}, J_{syn} = 7.2 Hz), 2.94 and 2.91 (2d, 4H, CHH_{anti}CHCHH_{anti}, J_{anti} = 12.2 Hz), 1.20 and 1.10 (2d, 12H, NCH(CH₃)₂, ³J_{H-H} = 6.3 Hz). ¹³C NMR (75 MHz, CDCl₃): δ 113.45 and 111.61 (allyl CH₂CHCH₂), 60.83 and 57.57 (allyl CH₂CHCH₂), 55.73 (NCH(CH₃)₂), 22.21 and 21.96 (NCH(CH₃)₂). Anal. Calcd for C₁₄H₂₄N₂S₂Pd₂: C, 33.81; H, 4.86; N, 5.63. Found: C, 33.72; H, 5.01; N, 5.68.

[(η³-Allyl)Pd]₂[μ-(benzyl)₂-DTO κ-N,N' Pd, κ-S,S' Pd'] (11). Yield: 0.37 gr (31.0%). ¹H NMR (300 MHz, CDCl₃): δ 7.34–7.17 (10H, NCH₂C₆H₆), 5.26 and 4.92 (2m, 2H, allyl CH₂CHCH₂), 5.23 and 5.22 (two AB spin systems, 4H, NCH₂–), 3.99 and 2.98 (2d, 4H, CHH_{syn}CHCHH_{syn}, J_{syn} = 7.00 Hz), 2.92 and 2.26 (2d, 4H, CHH_{anti}CHCHH_{anti}, J_{anti} = 12.82 Hz). ¹³C NMR (300 MHz, CDCl₃): δ 138.6, 128.4, 127.1, 126.7 (NCH₂C₆H₅), 114.5 and 113.7 (allyl CH₂CHCH₂), 68.25 and 64.17 (allyl CH₂CHCH₂), 62.14 (NCH₂–). Anal. Calcd for C₂₂H₂₄N₂S₂Pd₂: C, 44.53; H, 4.08; N, 4.72. Found: C, 44.31; H, 4.00; N, 4.80.

[(η³-Allyl)Pd]₂[μ-(isoamyl)₂-DTO κ-N,N' Pd, κ-S,S' Pd'] (12). Yield: 0.48 gr (43.2%). ¹H NMR (300 MHz, CDCl₃): δ 5.50 and 5.28 (2m, 2H, allyl CH₂CHCH₂), 4.00 and 3.56 (2d, 4H, CHH_{syn}CHCHH_{syn}, J_{syn} = 7.1 Hz), 3.93 (m, AB₂ spin system, 4H, NCH₂CH₂CH(CH₃)₂, 2.97 and 2.92 (2d, 4H, CHH_{anti}CHCHH_{anti}, J_{anti} = 12.6 Hz), 1.70 and 1.56 (2m, 6H, NCH₂CH₂CH(CH₃)₂, 0.97 (d, 12H, NCH₂CH₂CH(CH₃)₂, ³J_{H-H} = 6.6 Hz). ¹³C NMR (75 MHz, CDCl₃): δ 115.4 and 113.2 (allyl CH₂CHCH₂), 61.00 and 57.6 (allyl CH₂CHCH₂), 58.1 (NCH₂CH₂CH(CH₃)₂), 36.7 (NCH₂CH₂CH(CH₃)₂), 26.7 (NCH₂CH₂CH(CH₃)₂), 22.78 and 22.68 (NCH₂CH₂CH(CH₃)₂). Anal. Calcd for C₁₆H₂₈N₂S₂Pd₂: C, 36.58; H, 5.37; N, 5.33. Found: C, 36.61; H, 5.32; N, 5.39.

[(η³-Allyl)Pd]₂[μ-[(S)-1-(1-phenyl)ethyl]₂-DTO κ-N,N' Pd, κ-S,S' Pd'] (13). Yield: 0.23 gr (18.4%). ¹H NMR (300 MHz, CDCl₃): δ 7.42–7.21 (10H, NCH(CH₃)C₆H₆), 6.10 (m, 2H, NCH(CH₃)C₆H₆), 5.34 and 4.55 (2m, 2H, allyl CH₂CHCH₂), 4.04 (d, 2H, CHH_{syn}CHCHH_{syn}, near to sulfur atoms, J_{syn} = 6.8 Hz), 3.17 and 2.54 (2d, 2H, CHCH_{syn}CHCHCH_{syn}, near to nitrogen atoms, J_{syn} = 6.8 Hz), 2.97 (d, 2H, CHH_{anti}CHCHH_{anti}, near to sulfur atoms, J_{anti} = 12.6 Hz), 2.30 and 1.36 (2d, 2H, CHH_{anti}CHCHH_{anti}, near to nitrogen atoms, J_{anti} = 12.6 Hz). 1.66, 1.65, 1.57, 1.56 (4d, 6H, NCH(CH₃)C₆H₆, ³J_{H-H} = 6.6 Hz). ¹³C NMR (75 MHz, CDCl₃): δ 143.8, 128.09, 126.76, 126.70, 126.50 (NCH(CH₃)C₆H₅), 113.58, 111.65 (allyl CH₂CHCH₂), 61.57,

Scheme 1. Synthesis of $[(\eta^3\text{-Allyl})\text{Pd}]_2(\mu\text{-dialkyldithiooxamidate } \kappa\text{-N,S Pd, } \kappa\text{-N',S' Pd'})$ ComplexesChart 2. Stereoisomers of $[(\eta^3\text{-Allyl})\text{Pd}]_2(\mu\text{-dialkyldithiooxamidate } \kappa\text{-N,S Pd, } \kappa\text{-N',S' Pd'})$ with Their Stereochemical Descriptors

61.26, 58.10, 57.70 (allyl CH_2CHCH_2), 59.90 ($\text{NCH}(\text{CH}_3)\text{C}_6\text{H}_5$), 18.75 and 17.47 ($\text{NCH}(\text{CH}_3)\text{C}_6\text{H}_5$). Anal. Calcd for $\text{C}_{24}\text{H}_{28}\text{N}_2\text{S}_2\text{Pd}_2$: C, 46.38; H, 4.54; N, 4.51. Found: C, 46.39; H, 4.49; N, 4.63.

$[(\eta^3\text{-Allyl})\text{Pd}]_2[\mu\text{-}[\textit{meso}\text{-}(1\text{-phenyl)ethyl}]\text{-DTO } \kappa\text{-N,N' Pd, } \kappa\text{-S,S' Pd'}]$ (**14**). Yield: 0.27 gr (21.6%). $^1\text{H NMR}$ (300 MHz, CDCl_3): δ 7.35–7.13 (10H, $\text{NCH}(\text{CH}_3)\text{C}_6\text{H}_5$), 6.03 (m, 2H, $\text{NCH}(\text{CH}_3)\text{-C}_6\text{H}_6$), 5.30, 4.46, 4.20 (m, 2H, allyl CH_2CHCH_2), 4.06, 4.00, 4.00, 3.98, 3.13, 3.13, 2.49, 2.48 (8d, 4H, $\text{CHH}_{\text{syn}}\text{CHCHH}_{\text{syn}}$, $J_{\text{syn}} = 7.1$ Hz), 2.94, 2.94, 2.94, 2.92, 2.32, 2.32, 2.19, 2.18 (8d, 4H, $\text{CHH}_{\text{anti}}\text{CHCHH}_{\text{anti}}$, $J_{\text{anti}} = 12.5$ Hz), 1.61, 1.60, 1.50, 1.49 (4d, 6H, $\text{NCH}(\text{CH}_3)\text{C}_6\text{H}_6$, $^3J_{\text{H-H}} = 6.4$ Hz). $^{13}\text{C NMR}$ (75 MHz, CDCl_3): δ 143.60, 143.40, 128.50, 128.00, 126.80, 126.70, 126.60, 126.50 ($\text{NCH}(\text{CH}_3)\text{C}_6\text{H}_5$), 113.60, 112.10, 111.10 (allyl CH_2CHCH_2), 61.50, 61.30, 60.00 (allyl CH_2CHCH_2), 57.85, 57.80 ($\text{NCH}(\text{CH}_3)\text{C}_6\text{H}_5$), 18.05, 18.03, 17.12, 17.10 ($\text{NCH}(\text{CH}_3)\text{C}_6\text{H}_5$). Anal. Calcd for $\text{C}_{24}\text{H}_{28}\text{N}_2\text{S}_2\text{Pd}_2$: C, 46.38; H, 4.54; N, 4.51. Found: C, 46.41; H, 4.57; N, 4.55.

$[(\eta^3\text{-Allyl})\text{Pd}]_2[\mu\text{-}[\textit{rac}\text{-}(1\text{-phenyl)ethyl}]\text{-DTO } \kappa\text{-N,N' Pd, } \kappa\text{-S, S' Pd'}]$ (**15**). This compound was prepared exclusively for the purpose of growing X-ray-quality crystals. Its NMR spectra were identical with those of **13**. The yield and other analytical data were not determined.

RESULTS AND DISCUSSION

$\kappa\text{-N,S Pd, } \kappa\text{-N',S' Pd'}$ Coordination Mode. The reaction of $[(\eta^3\text{-allyl})\text{palladium}(\text{HR}_2\text{DTO } \kappa\text{-S,S Pd})]$ ($\text{HR}_2\text{DTO} = \text{N,N-dialkyldithiooxamidate}$; R = methyl, **1**; ethyl, **2**; isopropyl, **3**; benzyl, **4**; isoamyl, **5**) with $[(\eta^3\text{-allyl})\text{PdCl}]_2$ in a 2:1 ratio, performed in chloroform at 45 °C in 24 h, gave dimers in which two allylpalladium fragments are connected by a binucleating dithiooxamidate frame $\text{R}_2\text{DTO}^{2-}$ in an N,S coordination mode $[(\eta^3\text{-allyl})\text{palladium}]_2(\mu\text{-R}_2\text{DTO } \kappa\text{-N,S Pd, } \kappa\text{-N',S' Pd'})$ (Scheme 1).

The structural assignment is based on the $^1\text{H NMR}$ spectra of the new homobimetallic complexes, which are consistent with C_2 or C_i symmetry. In fact, the two allylpalladium frames connected as indicated above can point with the allyl cusps either to the same or to opposite sides of the mean plane of the molecule. These stereochemistries provide the bimetallic complex having C_i symmetry (exo isomer) and that having C_2 symmetry (endo isomer). The latter is chiral and, as such, should exist in solution as a racemate (Chart 2).

The stereochemistry of the above compounds can be properly described by taking into account that an allylpalladium frame linked to two different donor atoms defines a chiral plane. This chiral plane can be termed by means of A,C descriptors, which can easily be deduced by viewing the molecule from the central allyl carbon toward palladium.^{2,11} In such a view, the other two atoms coordinated to the metal, sulfur and nitrogen, follow a clockwise direction based on decreasing CIP priority in C, whereas these atoms follow the anticlockwise direction in A. The chirality in allylpalladium complexes has been envisaged by other authors as a central chirality and, as such, has been indicated by means of R,S descriptors.²⁰ Regardless of the nomenclature, each enantiomer of endo isomers has its palladium centers in the same configuration, while the exo isomer is a meso form in which the palladium centers have opposite configurations.

$^1\text{H NMR}$ spectra of $[(\eta^3\text{-allyl})\text{palladium}]_2(\mu\text{-R}_2\text{DTO } \kappa\text{-N,S Pd, } \kappa\text{-N',S' Pd'})$ bimetallic compounds (R = methyl, **1**; ethyl, **2**; isopropyl, **3**; benzyl, **4**; isoamyl, **5**) show only one set of signals, i.e., a multiplet for the central allyl proton, two doublets for $-\text{CHH}_{\text{syn}}-$ and two doublets for $-\text{CHH}_{\text{anti}}-$ allyl protons, and the expected resonances for the given alkyl group. These are the spectral feature that can be expected for a bimetallic compound having C_2 or C_i symmetry.

When two allylpalladium moieties are bridged by symmetrical binucleating ligands²¹ and the motion of the allyl unit is slow on the NMR time scale, both endo and exo isomers can be observed.

We can be confident that both isomers can exist in solution at room temperature because NCH_2- protons in ethyl, isoamyl, and benzyl groups appear as ABX_3 , ABX_2 , and AB spin systems, respectively. Furthermore, resonances of the geminal methyl units in isopropyl and isoamyl groups are split, meaning that a fast allyl pseudorotation can reasonably be ruled out. For this reason, we found it surprising that diastereomers like those depicted in Chart 1 could show coincident NMR resonances. We therefore attempted to detect both C_2 - and C_i -symmetrical isomers in solution by using chiral auxiliaries as substituents of the binucleating DTO. We prepared the binuclear complexes $[(\eta^3\text{-allyl})\text{palladium}]_2[\mu\text{-}[\textit{1-(S)-(1-phenylethyl)}]\text{-DTO } \kappa\text{-N,S Pd, } \kappa\text{-N',S' Pd'}]$ (**6**) and $[(\eta^3\text{-allyl})\text{palladium}]_2[\mu\text{-}[\textit{meso}\text{-}[(1\text{-phenyl)ethyl}]\text{-DTO } \kappa\text{-N,S Pd, } \kappa\text{-N',S' Pd'}]$ (**7**) following the above-reported synthetic procedure using the chiral N,N-bis[1-(S)-(1-phenylethyl)]dithiooxamidate and the corresponding

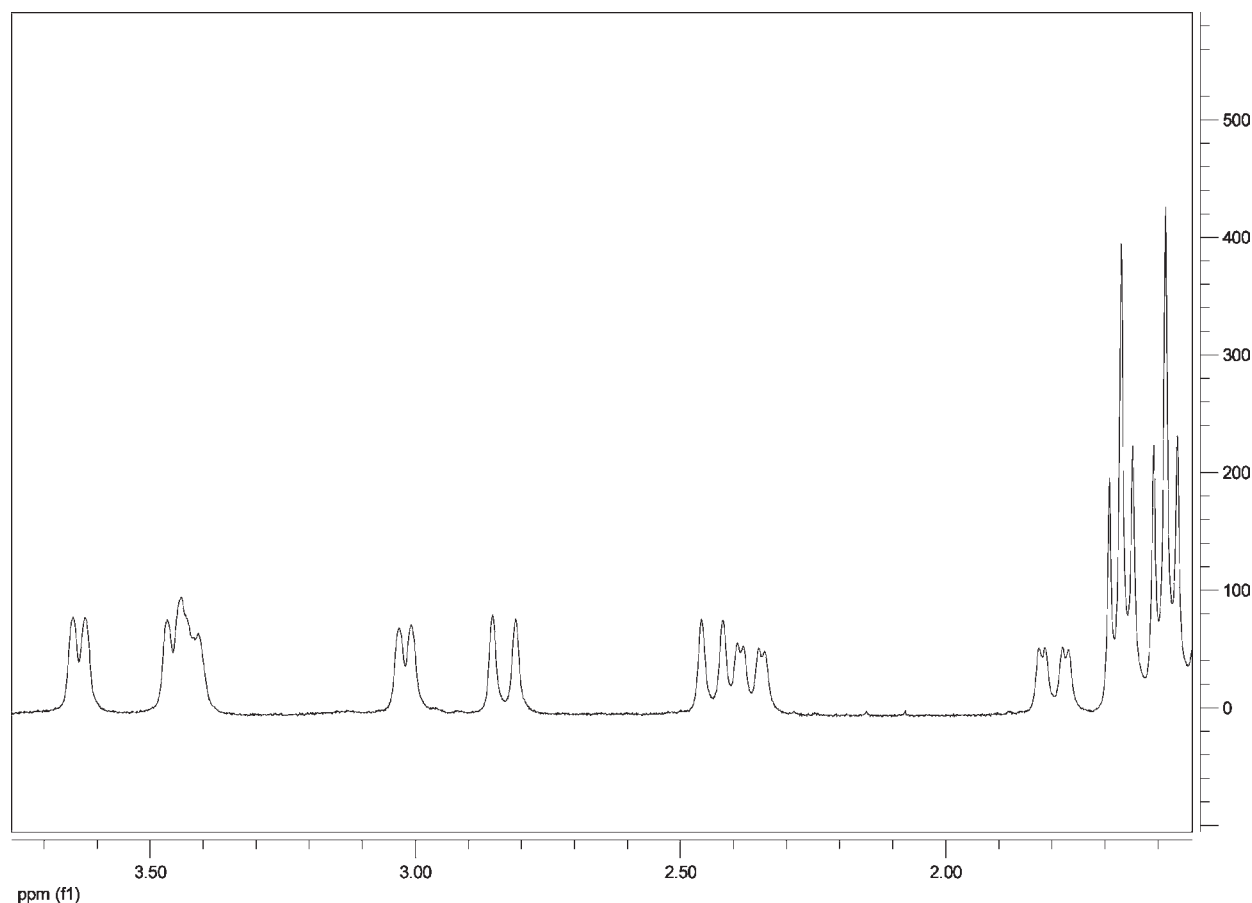


Figure 1. ^1H NMR spectrum of **6**. The spectrum of **7** is identical.

achiral meso form N -[1-(*S*)-1-phenylethyl]- N' -[1-(*R*)-1-phenylethyl]dithiooxamide, respectively.

Both syntheses gave two isomeric mixtures that show identical NMR spectra where 2:4:2 allyl $-\text{CHH}_{\text{syn}}$ doublets, 2:2:1:1:1:1 allyl CHH_{anti} doublets, and four equally intense $\text{NCH}(\text{CH}_3)\text{-C}_6\text{H}_5$ doublets are easily detectable (Figure 1).

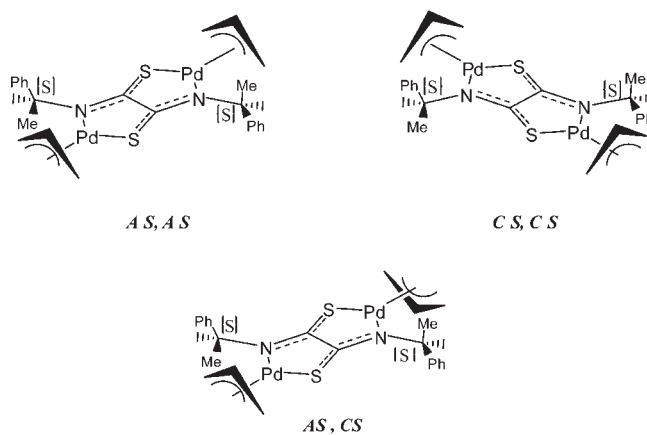
The observed spectra account for both chiral (**6**) and achiral (**7**) diastereomers.

Indeed, $[(\eta^3\text{-allyl})\text{palladium}]_2[\mu\text{-}[1\text{-}(S)\text{-}(1\text{-phenylethyl})]_2\text{D-T-O } \kappa\text{-N,S Pd, } \kappa\text{-N',S' Pd}']$ may exist as the isomeric mixture shown in Chart 3.

The above chart depicts three diastereomers, labeled *AS,AS*, *CS,CS*, and *AS,CS*. In *AS,AS* and *CS,CS*, a C_2 axis connects the two $(\eta^3\text{-allyl})\text{Pd}(\text{RNCS})-$ fragments; hence, each of them shows only one group of signals in the ^1H NMR, i.e., two doublets (syn protons), two doublets (anti protons), and last one doublet (methyl groups). In contrast, in the *AS,CS* stereoisomer, the $(\text{allyl})\text{Pd}(\text{RNCS})-$ halves are diastereotopic; hence, each half of the molecule has its own set of signals. In the ^1H NMR spectrum, the four groups of signals have the same intensity, indicating that the three isomers have formed with the expected statistical ratio (25, 25, and 50%).

As stated above, $[(\eta^3\text{-allyl})\text{Pd}]_2[\mu\text{-}(meso\text{-}(1\text{-phenyl)ethyl})]_2\text{D-T-O } \kappa\text{-N,S Pd, } \kappa\text{-N',S' Pd}']$ also shows the same ^1H NMR spectrum of the corresponding chiral compound. Despite their very close similarity, the two spectra have a different stereochemical meaning. In fact, the above symmetric meso compound is a mixture of the isomers: indicated in Chart 4,

Chart 3. Stereoisomers of $[(\eta^3\text{-Allyl})\text{Pd}]_2[\mu\text{-}[1\text{-}(S)\text{-}(1\text{-phenylethyl})]_2\text{dithiooxamidate } \kappa\text{-N,S Pd, } \kappa\text{-N',S' Pd}']$ with Their Stereochemical Descriptors

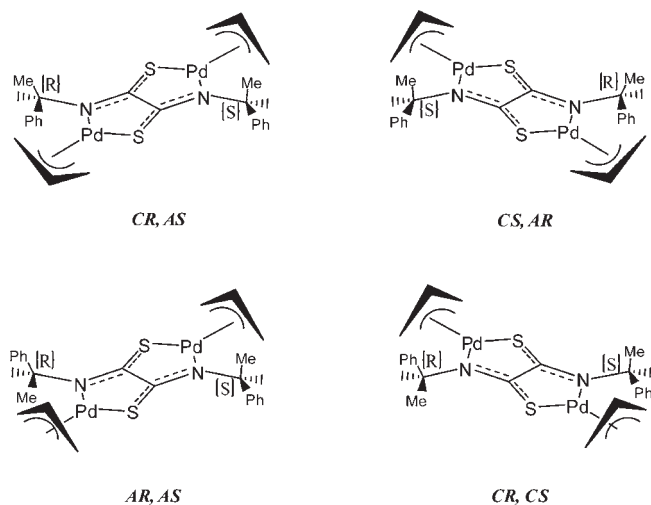


CR,AS and CS,AR are two C_2 -symmetrical meso forms; each one is constituted by enantiotopic halves rotated 180° with respect to the inversion center. Clearly, the stereochemistry of the above compounds arises from the two different ways in which two enantiotopic carbon atoms can be placed with respect to the enantiotopic half-spaces; according to Prelog and Helmchen, this is pseudoasymmetry.^{22,23} We already pointed out that pseudoasymmetry should be viewed as an important issue in inorganic

stereochemistry because the great variety of coordination geometries can supply a number of compounds constituted by enantiotopic halves.¹¹

CR,AS and CS,AR isomers are a new variety of inorganic pseudochiral compounds. In fact, pseudoasymmetry, observed in

Chart 4. Stereoisomers of $[(\eta^3\text{-Allyl})\text{Pd}]_2[\mu\text{-}meso\text{-}(1\text{-phenyl})\text{-ethylthiooxamidate } \kappa\text{-N,S Pd, } \kappa\text{-N',S' Pd}']$ with Their Stereochemical Descriptors



C_s -symmetric metal complexes sporadically,^{9,11,24,25} is here reported for the first time in a C_i -symmetric organometallic molecule. The remaining pair of isomers, AR,AS and CR,CS , constitute an enantiomeric pair.

The ^1H NMR spectrum of $[(\eta^3\text{-allyl})\text{Pd}]_2[\mu\text{-}meso\text{-}(1\text{-phenyl})\text{-ethyl}]_2\text{DTO } \kappa\text{-N,S Pd, } \kappa\text{-N',S' Pd}'$ features well the isomeric mixture described above. In fact, each pseudochiral isomer shows its own set of signals, while the $AR,AS/CR,CS$ pair has two sets of signals because each enantiomer is constituted by diastereotopic halves. The four sets of signals in the meso compounds also show the same intensity with respect to one another because each isomer exists in solution in the expected statistical ratio, i.e., 25% (AR,CS), 25% (AS,CR), and 50% ($AR,AS/CR,CS$).

Bidimensional NOESY spectra of both $[(\eta^3\text{-allyl})\text{palladium}]_2\text{-}(\mu\text{-}meso\text{-phenylethyl})_2\text{DTO } \kappa\text{-N,S Pd, } \kappa\text{-N',S' Pd}'$ and $[(\eta^3\text{-allyl})\text{-palladium}]_2[1\text{-}(S)\text{-}(1\text{-phenylethyl})]_2\text{DTO } \kappa\text{-N,S Pd, } \kappa\text{-N',S' Pd}'$ are identical (Figure 2). In particular, in both spectra, there are opposite phase cross peaks between allyl and the DTO resonances of the various diastereomers of which homobimetallic complexes are made.

As for the allyl resonances, syn–syn and anti–anti exchanges were observed. This clearly indicates that allyl pseudorotation occurs in solution, which changes the diastereomers into one another. The observed exchanges are consistent with a mechanism that involves dissociation of the Pd–N bond. We previously proposed a similar mechanism for other binuclear and trinuclear metal complexes containing a palladium allyl moiety linked to a

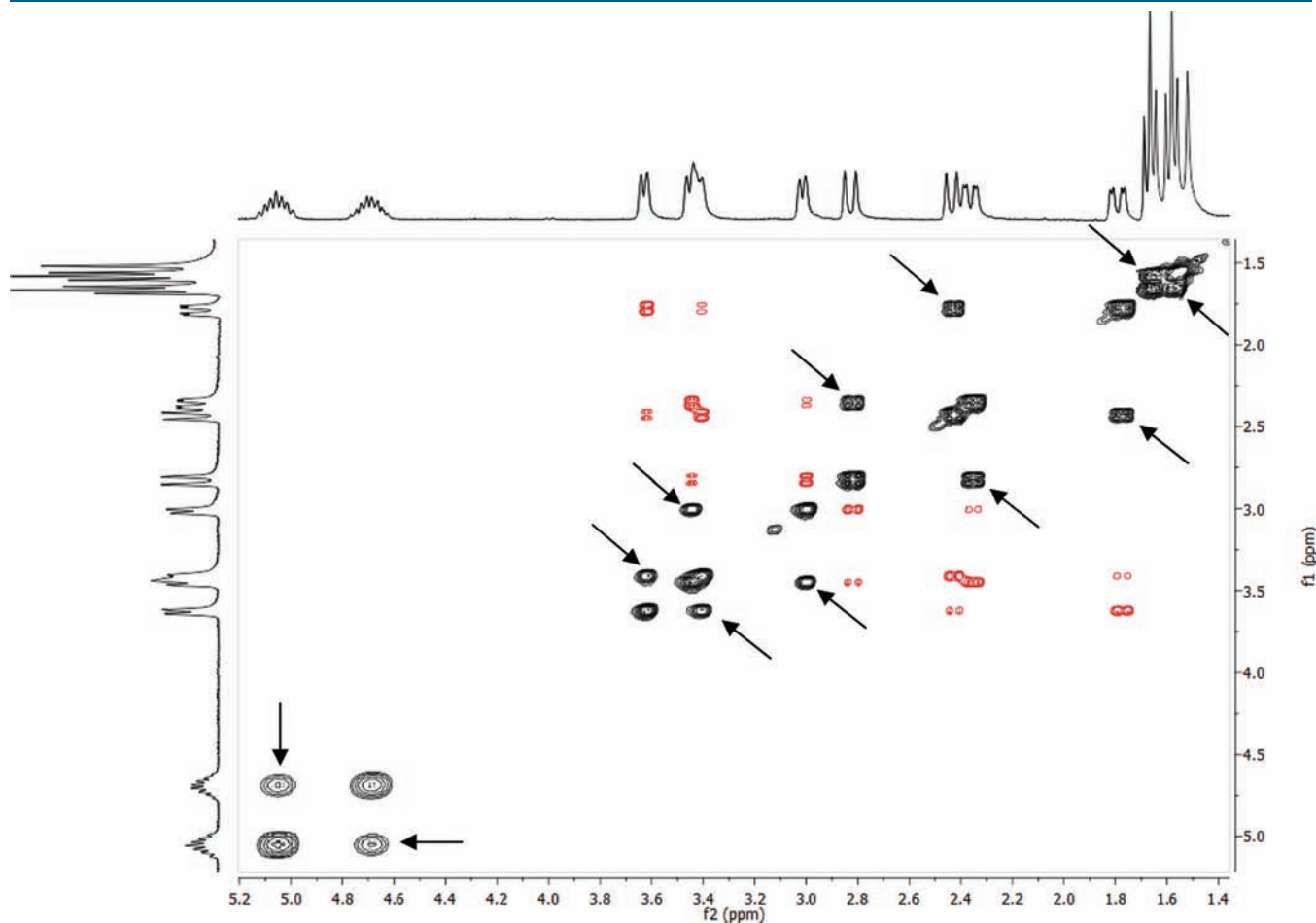
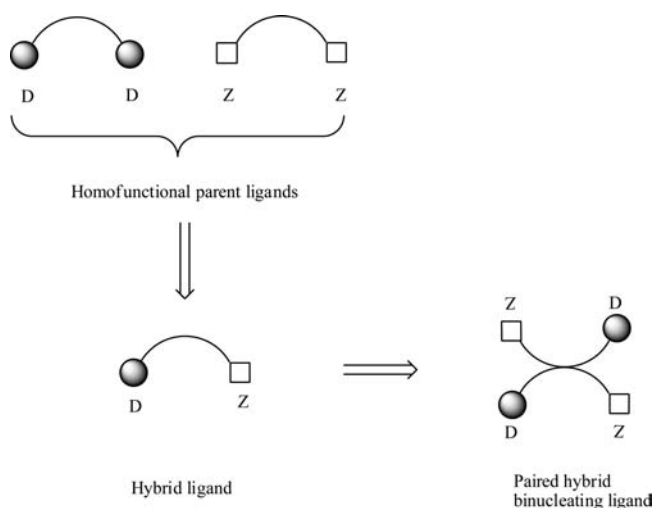


Figure 2. Bidimensional EXSY spectrum of **6**. Exchange cross peaks are indicated by arrows. The spectrum of **7** is identical.

Scheme 2. Hybrid Binucleating Ligand Containing Two Chemically Different Donor Functions



nitrogen chelating system.^{2,3} This happens because a hard ligand—soft metal interaction is produced when an allyl fragment is bound by means of a homofunctional N[^]N-chelating system. Such an unfavourable interaction allows the Pd–N bond to break, and this is the first step of the proposed allyl pseudorotation mechanism. At the same time, we were able to demonstrate that allyl pseudorotation is not observed when an allylpalladium frame is linked to a sulfur-chelating system.² After all, when a (η^3 -allyl)palladium frame is bound to a homofunctional S[^]S chelating system (i.e., a soft donor system bound to a soft metal), the resulting soft ligand–soft metal strong interaction does not allow the Pd–S bond to break, and as a result, allyl pseudorotation is not observed.

In the above homobimetallic complexes, two allylpalladium fragments are joined to each other by a secondary DTO in an N,S coordination mode. When linked in such a way, the binucleating DTO behaves as a double-hybrid ligand.

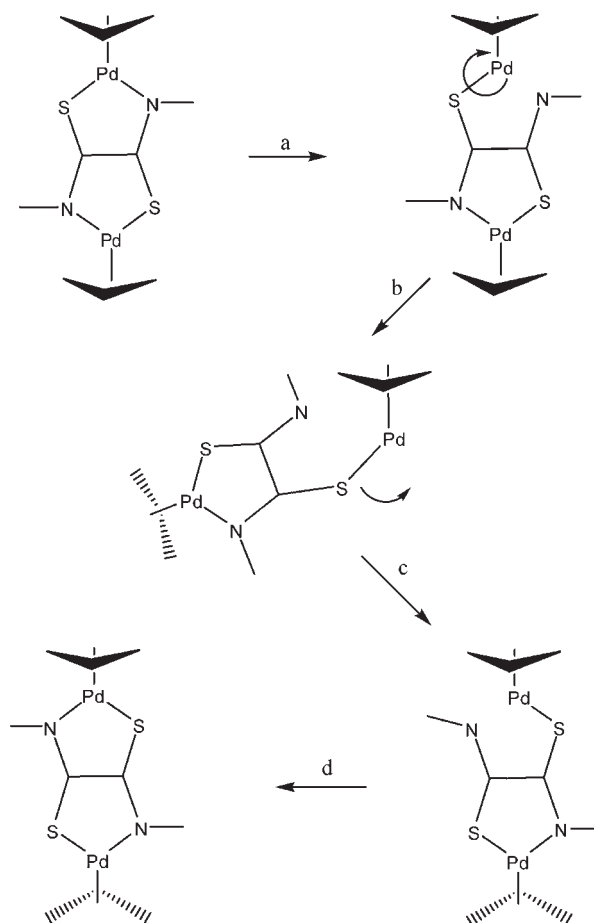
A hybrid ligand is a polydentate ligand that contains at least two different types of chemical functionalities capable of binding to metal centers (Scheme 2). Although it may be considered as being derived from a pair of homofunctional ligands, its properties are new compared to either of its parent compounds.²⁶ Such ligands, either chelating or binucleating, can be represented by the formalism proposed by Braunstein.²⁷

Hybrid ligands are closely linked to the concept of hemilability, which refers to systems containing at least one substitutionally labile donor function Z while the other donor group D remains firmly bound to the metal. The term “hemilabile” was first used to indicate phosphine–amine and phosphine–ether ligands, which would bind a given metal but would readily dissociate the “hard” ligand component.²⁸ However, the phenomenon itself had been observed earlier.²⁹

Thus, a DTO frame linked to two allylpalladium moieties in an N,S coordination mode undergoes dissociation of one hard ligand component, i.e., the amidic nitrogen (step a in Scheme 3); then a rotation around the Pd–S bond takes place (step b); after that, isomerization of the T-shaped intermediate occurs (step c), followed by the remaking of the Pd–N bond (step d).

Isomerization processes of allylpalladium mononuclear complexes bearing P[^]N,^{20b,30–32} C[^]N,³³ P[^]PS,^{20a,34} P[^]PO,³⁵ N[^]S,³⁶ and N[^]O³⁷ hemilabile ligands have been widely studied. The

Scheme 3. Proposed Mechanism for Apparent Allyl Rotation in $[(\eta^3\text{-allyl})\text{Pd}]_2(\mu\text{-dialkyldithiooxamidate } \kappa\text{-N,S Pd, } \kappa\text{-N', S' Pd}')$



present report shows the allyl isomerization process in two allylpalladium moieties binucleated by coupled hemilabile N[^]S pairs; in both (η^3 -allyl)Pd(N[^]S)– fragments, the allyl motion seems to take place through the κ^1 form of the hemilabile N[^]S-chelating system.³⁸

$\kappa\text{-N,N' Pd, } \kappa\text{-S,S' Pd'}$ Coordination Mode. By reacting $[(\eta^3\text{-allyl})\text{palladium}(\text{HR}_2\text{DTO } \kappa\text{-S,S Pd})]$ ($\text{HR}_2\text{DTO}^- = \text{N,N'}$ -dialkyldithiooxamidate; R = methyl, **8**; ethyl, **9**; isopropyl, **10**; benzyl, **11**; isoamyl, **12**) with $[(\eta^3\text{-allyl})\text{PdCl}]_2$ in a 2:1 ratio, in chloroform at 20 °C for $1/2$ h, the following process takes place: the binuclear complexes $[(\eta^3\text{-allyl})\text{Pd}]_2(\mu\text{-R}_2\text{DTO } \kappa\text{-N,N' Pd, } \kappa\text{-S,S' Pd'})$ (R = methyl, **8**; ethyl, **9**; isopropyl, **10**; benzyl, **11**; isoamyl, **12**) are formed in moderate yield (Scheme 4).

¹H NMR spectra of complexes **8–12** show two distinct allyl systems, each constituted by three physically associated signals (NOE cross peak in the bidimensional spectra), i.e., a complex multiplet (central CH), a lower ³J doublet (CHH_{syn}), and a higher ³J doublet (CHH_{anti}). Obviously, one of the two allyl spin systems refers to the ($\eta^3\text{-C}_6\text{H}_5$)Pd(N[^]N)– fragment, the other to the ($\eta^3\text{-C}_6\text{H}_5$)Pd(S[^]S)– group. Alkyl resonances also appear as a single group of signals because of the C_s symmetry of the new complexes.

Two stereomers having C_s symmetry could account for the observed NMR spectra; one of these has both allyl cusps directed toward the same side of the molecular plane (endo in

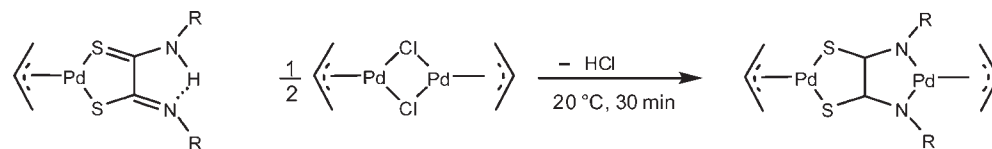
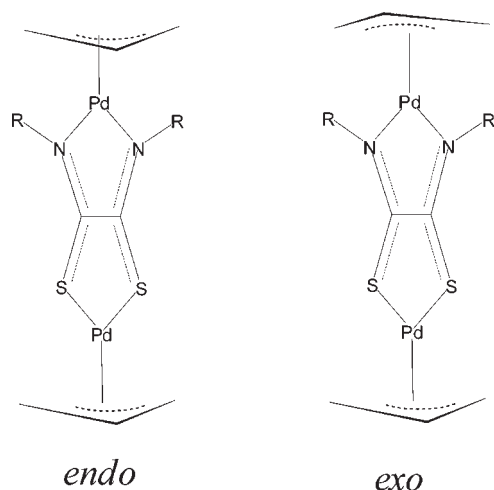
Scheme 4. Synthesis of $[(\eta^3\text{-Allyl})\text{Pd}]_2(\mu\text{-dialkyldithiooxamidate } \kappa\text{-S,S}' \text{ Pd } \kappa\text{-N,N}' \text{ Pd}')$ ComplexesChart 5. Stereoisomers of $[(\eta^3\text{-Allyl})\text{Pd}]_2(\mu\text{-dialkyldithiooxamidate } \kappa\text{-N,N}' \text{ Pd}, \kappa\text{-S,S}' \text{ Pd}')$ Species

Chart 5) and the other having allyl CH pointed toward opposite sides of the said plane (exo in Chart 5). The geminal hydrogen atoms in the methylene groups of **9**, **11**, and **12**, as well as the geminal methyl groups in **10**, are diastereotopic. This means that the allyl isomerization processes are of high energy, thus allowing both isomers to exist in solution.

We found it surprising that diastereomers like those depicted in Chart 5 could show coincident NMR resonances. We therefore attempted to detect the two C_s -symmetrical isomers using chiral auxiliaries as substituents in the binucleating DTO.

We synthesized the binuclear complex $[(\eta^3\text{-allyl})\text{Pd}]_2[\mu\text{-[1-(S)-(1-phenylethyl)]}_2\text{DTO } \kappa\text{-N,N}' \text{ Pd}, \kappa\text{-S,S}' \text{ Pd}']$ (**13**) and $[(\eta^3\text{-allyl})\text{Pd}]_2[\mu\text{-[meso-(1-phenyl)ethyl]}_2\text{-DTO } \kappa\text{-N,N}' \text{ Pd}, \kappa\text{-S,S}' \text{ Pd}']$ (**14**).

The ^1H NMR spectrum of **13** shows two groups of signals; the first, near the sulfur-chelating system, contains a multiplet (central CH) and two doublets (syn and anti protons) in a 1:2:2 ratio. The other, near the nitrogen donor atoms, shows a central CH multiplet, two doublets, and two CHH_{anti} doublets in a 1:1:1:1:1 ratio. Lastly, four equally intense doublets are due to the methyl groups of the phenylethyl substituents.

The observed resonances are assigned to the two diastereomers like those depicted in Chart 5 when $R = 1\text{-}(S)\text{-1-phenylethyl}$; in the spectrum, the allyl resonances of the two stereoisomers are isochronous, while syn and anti protons of the allyl system near the nitrogen atoms appear as split doublets because of the presence of two homochiral substituents opposite to each other with respect to the symmetry plane of a C_s molecular skeleton.

The ^1H NMR spectrum of **14** exhibits two groups of signals for the allyl protons. The one that refers to the $(\eta^3\text{-C}_3\text{H}_5)\text{Pd}(\text{S}^{\wedge}\text{S})$ -fragment is constituted by a multiplet (central CH), four equally

intense doublets due to the syn protons (clearly distinguishable although very close to one another), and two doublets due to the anti protons (3:1 intensity); the other is made of two central allyl CH multiplets, three 2:1:1 (syn protons), and three 2:1:1 doublets (anti protons) and refers to the $(\eta^3\text{-C}_3\text{H}_5)\text{Pd}(\text{N}^{\wedge}\text{N})$ -fragment. Finally, four equally intense doublets are observed for the methyl protons of the phenylethyl groups. This spectrum is consistent with the presence, in solution, of the four stereoisomers of compound **14** (Chart 6).

Both endo and exo isomers have a C_s -symmetrical skeleton, and therefore they are constituted by enantiotopic halves. In each of these isomers, two enantiomeric groups can be positioned in two different ways, allowing two couples of diastereomeric meso forms to be formed.

With regards to the stereochemical descriptors for such stereoisomers, we suggest the terms endo/exo to indicate the reciprocal position of the allyl cuspid (Chart 5). The above endo and exo forms exist as two pseudochiral diastereomers that can be termed according to the procedures proposed previously.¹¹ Thus, the pseudochiral isomers c have the substituent 1-(R)-(1-phenyl)ethyl on the left-hand side with respect to the nearest allyl cuspid, while the corresponding a isomers have the substituent 1-(R)-(1-phenyl)ethyl on the right-hand side with respect to the same reference point.

Bidimensional EXSY spectra of **13** show NOE cross peaks between DTO hydrogen atoms and syn, but not anti, allyl protons (Figure 3).

This allows the allyl protons near the nitrogen-chelating system to be distinguished from those near the sulfur atoms. Analogous selective NOEs for allyl derivatives have been reported by Pregosin et al. and attributed to the CH syn twisting toward the metal out of the allyl plane.³⁹ *Syn-syn* and *anti-anti* exchange cross peaks were not observed. However, this does not rule out the allyl pseudorotation in the $(\eta^3\text{-C}_6\text{H}_5)\text{Pd}(\text{N}^{\wedge}\text{N})$ -fragment; in fact, exchange cross peaks between the syn and anti doublets cannot be observed because the resonances of syn and anti protons are isochronous in the two stereoisomers. The allyl pseudorotation in the $(\eta^3\text{-C}_6\text{H}_5)\text{Pd}(\text{N}^{\wedge}\text{N})$ -fragment of **13** is, however, documented by the presence of exchange cross peaks between the methyl doublets of the phenylethyl substituents. This allyl rearrangement that interconverts the two stereomeric forms of **13** arises from dissociation of a Pd–N bond in the $(\eta^3\text{-C}_6\text{H}_5)\text{Pd}(\text{N}^{\wedge}\text{N})$ -fragment.

The κ' form of the $\text{N}^{\wedge}\text{N}$ donor system is not anticipated to contribute in any way to endo/exo isomerization. Indeed, neither in mononuclear $[(\eta^3\text{-allyl})\text{Pd}(\text{H-meso-(1-phenyl)ethyl-DTO } \kappa\text{-S,S Pd})]^2$ nor in binuclear $[(2\text{-phenylpyridine})\text{Rh}(\mu\text{-isoamyl-DTO } \kappa\text{-N,N Rh } \kappa\text{-S,S Pd})\text{Pd}(\eta^3\text{-allyl})]$,¹⁰ which contain similar $\kappa\text{-S,S Pd}$ systems, has allyl movement been observed.

Again in the EXSY spectrum of **14**, NOE cross peaks allow the allyl system signals near sulfur atoms to be groups and enable them to be distinguished from the ones near the nitrogen-chelating system (Figure 4).

Chart 6. Stereoisomers of 14 with Their Stereochemical Descriptors

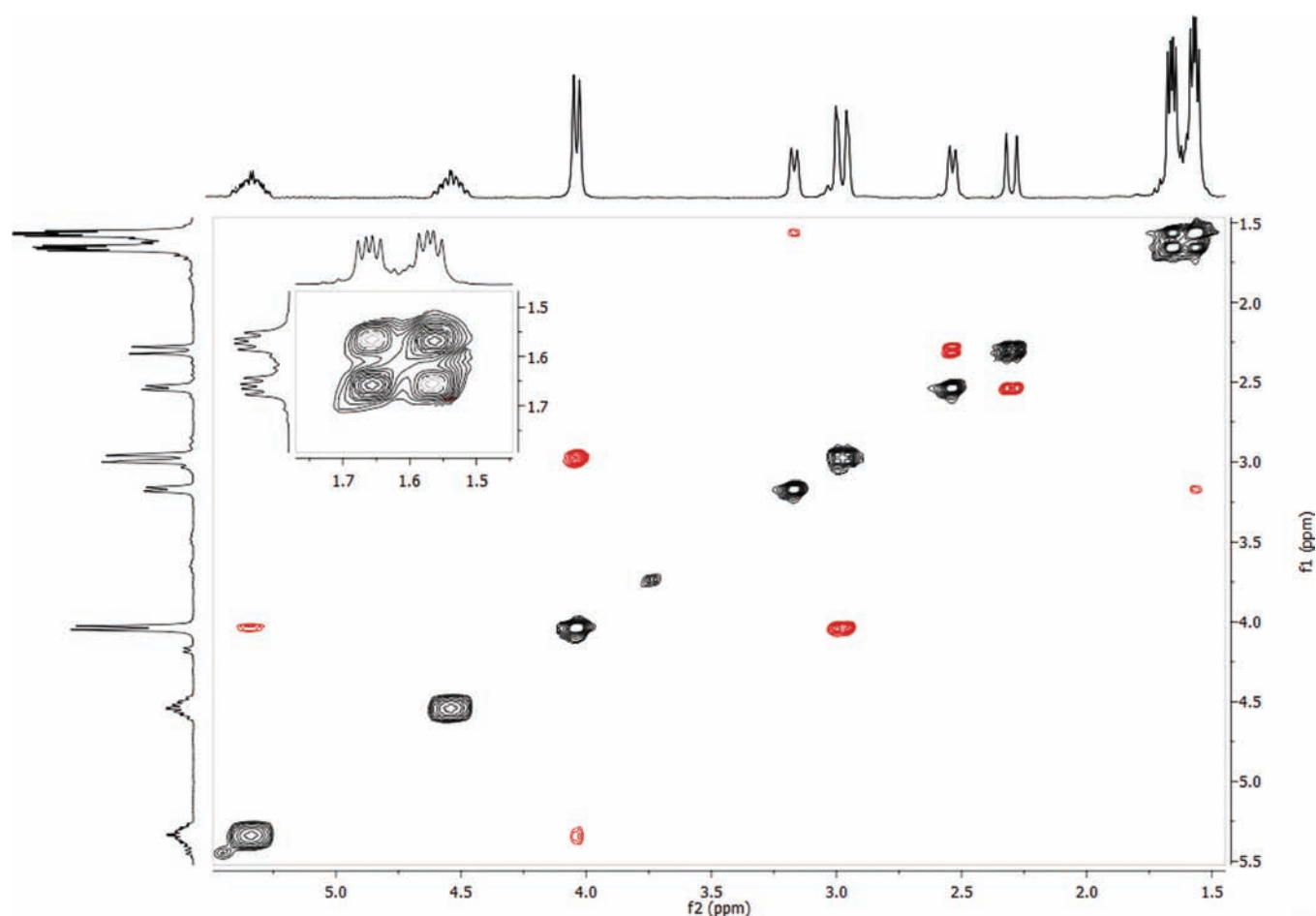
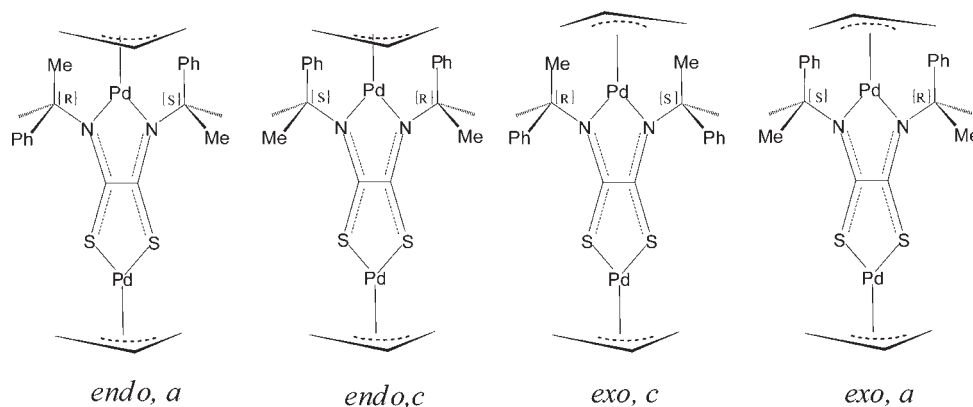


Figure 3. Bidimensional EXSY spectrum of 13. Exchange cross peaks due to the methyl groups signals are evidenced by the expansion.

Allyl hydrogen atoms close to the N[^]N group are well separated so that exchange cross peaks can easily be detected between the multiplets because of the central CH and the doublets of *syn* hydrogen atoms and *anti* hydrogen atoms. Once again, the *syn*–*syn* and *anti*–*anti* exchanges are consistent with an allyl pseudorotation mechanism, which involves (a) dissociation of one Pd–N bond, (b) rotation around the remaining Pd–N bond, (c) isomerization of the T-shaped intermediate, and (d) reforming of the Pd–N bond.²

As stated earlier, an essential feature of hemilabile ligands is to have at least one substitutionally labile donor function while the other donor group(s) remain firmly bound to the metal center(s). This condition is certainly met by the binucleating DTO in the κ -N,S coordination mode (complexes 1–7).

However, the concept of hemilability cannot be extended to dinuclear complexes such as 8–14. In fact, these compounds could be regarded as being formed from a complex as a ligand (frame A in Chart 7) and by a complex as a metal (frame B in Chart 7).

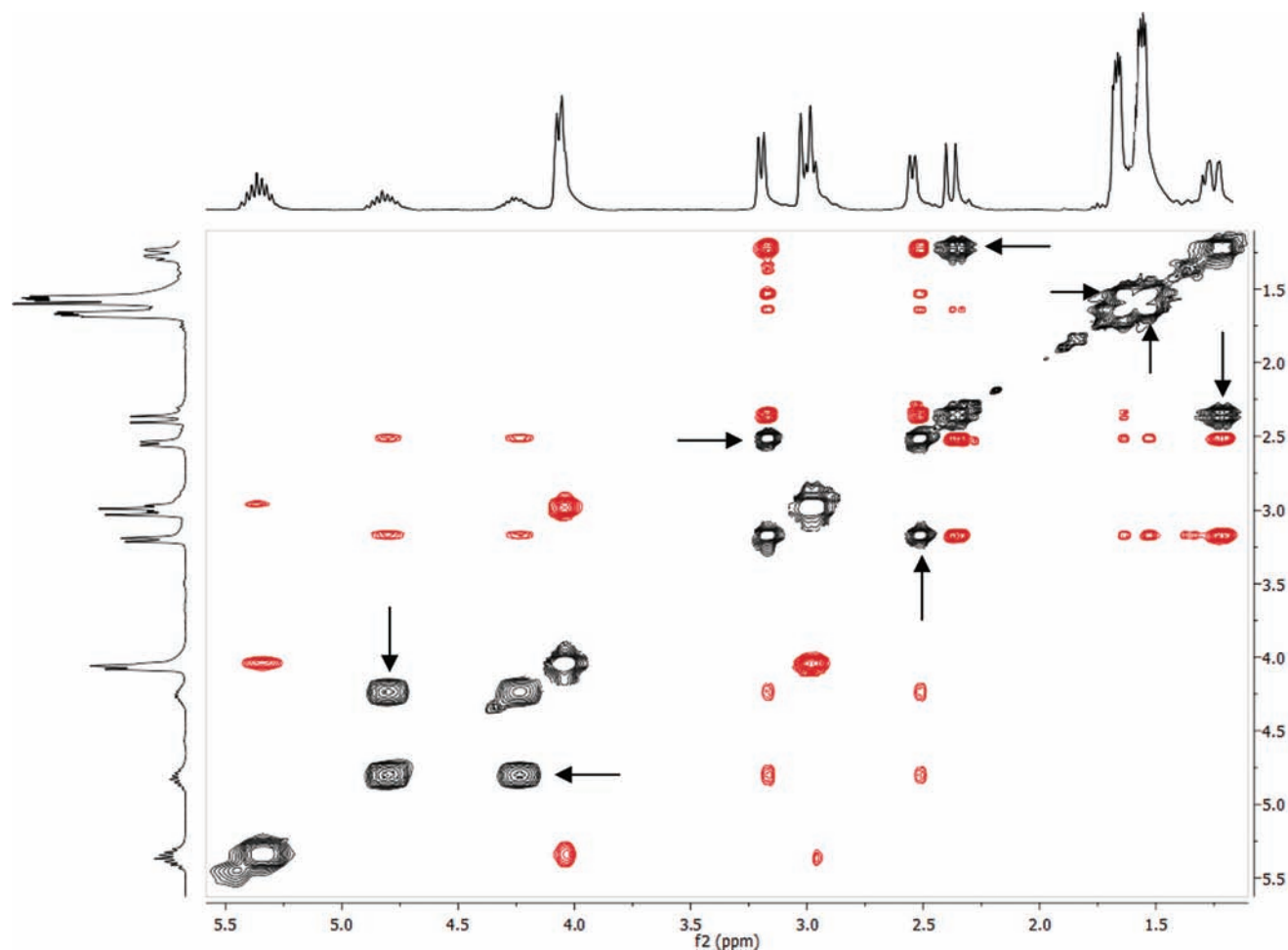
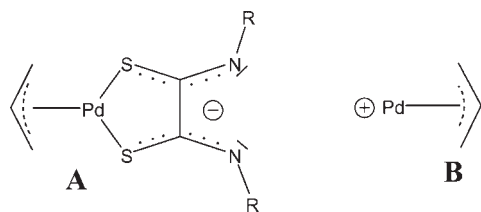


Figure 4. Bidimensional EXSY spectrum of 14. Exchange cross peaks are indicated by arrows.

Chart 7. $[\eta^3\text{-Allyl}]\text{Pd}]_2(\mu\text{-dialkyldithiooxamidate } \kappa\text{-S,S}' \text{ Pd } \kappa\text{-N,N}' \text{ Pd}')$ Complexes Viewed as Being Made by a Complex as a Ligand and a Complex as a Metal (See the Text)



From this point of view, A does not contain a hybrid hemilabile ligand but simply a homofunctional chelating system.

At this point, it is necessary to consider that when species 8–14 are left in solution, they undergo the following rearrangement shown in Scheme 5. The above process shows a half-life of about 1 day, depending on the nature of the alkyl substituents of 8–14; this is in agreement with the preparative separation of the two isomers and with their characterization in solution without mutual interference.

Detailed studies will be needed to assess the mechanism of the rearrangement of the binucleating ligand in the $\kappa\text{-N,N } \kappa\text{-S,S}'$ homobimetallic complexes 8–14.

At this stage, we can only argue that the change in the coordination mode of the ligand implies the breaking of the Pd–S bond in the $(\eta^3\text{-allyl})\text{Pd}(\text{S}^{\wedge}\text{S})$ frame. $[(\eta^3\text{-Allyl})\text{Pd}]_2(\mu\text{-R}_2\text{-DTO } \kappa\text{-N,N}' \text{ Pd}, \kappa\text{-S,S}' \text{ Pd}')$ species contain the $(\eta^3\text{-allyl})\text{Pd}(\text{N}^{\wedge}\text{N})$ frame in which the labile Pd(N \wedge N) interaction allows the apparent allyl rotation via Pd–N bond rupture; in the other frame, a more stable Pd(S \wedge S) interaction requires more energy to produce the rearrangement of the binucleating ligand via Pd–S bond rupture.

The change in the coordination mode of the binucleating ligands in complexes 8–14 was not surprising, in that both groups of compounds 1–7 and 8–14 were obtained via the same chemical reaction (Schemes 1 and 4), albeit performed in different experimental conditions. Compounds 1–7 were synthesized under thermodynamic control (higher temperature and longer reaction time), while the corresponding isomers 8–14 were prepared under kinetic control (lower temperature and shorter reaction time).

The spontaneous transformation of the $\kappa\text{-N,N}' \text{ Pd}, \kappa\text{-S,S}' \text{ Pd}'$ species (8–14) into the corresponding $\kappa\text{-N,S } \text{Pd}, \kappa\text{-N}' \text{ Pd}'$ ones (1–7) is mainly ruled by the stability of the thermodynamic compounds with respect to the kinetic ones.

The thermodynamic stability of metal–ligand interaction (HSAB principle)⁴⁰ is a well-assessed issue. Furthermore, because chemical hardness is related to the highest occupied

Scheme 5. Spontaneous Transformation of $[(\eta^3\text{-Allyl})\text{Pd}]_2(\mu\text{-dialkyldithiooxamidate } \kappa\text{-N,N}' \text{ Pd}, \kappa\text{-S,S Pd}')$ in the Corresponding $\kappa\text{-N,S Pd } \kappa\text{-N}',\text{S}' \text{ Pd}'$ Isomers

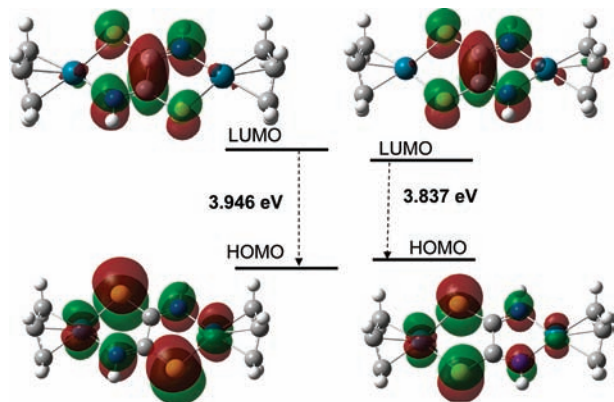
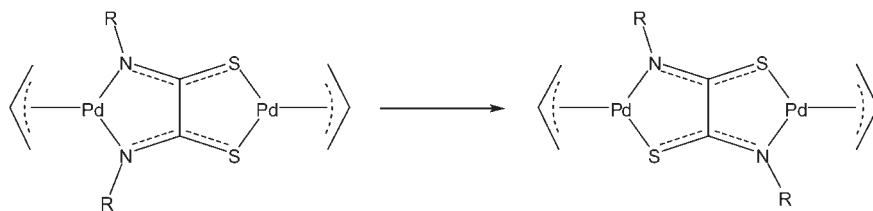


Figure 5. Electronic structures of model systems.

molecular orbital (HOMO)/lowest unoccupied molecular orbital (LUMO) gap of a molecular species as half the energy gap of the two orbitals [$\eta = (E_{\text{LUMO}} - E_{\text{HOMO}})/2$], the molecular stability can be evaluated using the maximum hardness principle, which states that molecules arrange themselves to be as hard as possible.⁴¹

We therefore performed theoretical calculations on a simplified model of both groups of complexes 1–7 and 8–14 in which a hydrogen atom was placed as the substituent on the amidic nitrogen atoms instead of the alkyl groups.

In the model system of molecules 8–14 ($\kappa\text{-N,N}' \text{ Pd}, \kappa\text{-S,S}' \text{ Pd}'$), we found that the HOMO–LUMO gap is 3.837 eV, while this gap is 3.946 eV for compounds 1–7 ($\kappa\text{-N,S Pd}, \kappa\text{-N}',\text{S}' \text{ Pd}'$). The larger gap for the latter compounds indicates that $\kappa\text{-N,S Pd}, \kappa\text{-N}',\text{S}' \text{ Pd}'$ species are the harder isomers. The harder isomers are more stable, and this fact matches with the greater stability (9.47 kcal) computed for the $\kappa\text{-N,S}$ isomer with respect to the corresponding $\kappa\text{-N,N } \kappa\text{-S,S}$ species.

The electronic structures of model systems (Figure 5) show that the LUMOs have a similar composition, which can be described as a p_z^* system of the NSC–CSN frame in both the $\kappa\text{-N,S}$ and $\kappa\text{-N,N } \kappa\text{-S,S}$ isomers. In contrast, HOMOs for the two isomeric models are quite different in composition from each other. In the $\kappa\text{-N,S}$ model, the HOMO is mainly formed by a combination of the p_z atomic orbital of nitrogen and sulfur atoms and the d_{xy} orbital of both palladium atoms, while in the $\kappa\text{-N,N } \kappa\text{-S,S}$ model, the contribution of the d_{xy} orbital in $\kappa\text{-N,N}$ palladium atom is somewhat lower.

The point we highlight is how a functional choice of hard–soft-donor chelating ligands can direct inorganic syntheses toward isomeric preferences^{42,43} or toward self-assembled molecular square architectures.⁴⁴

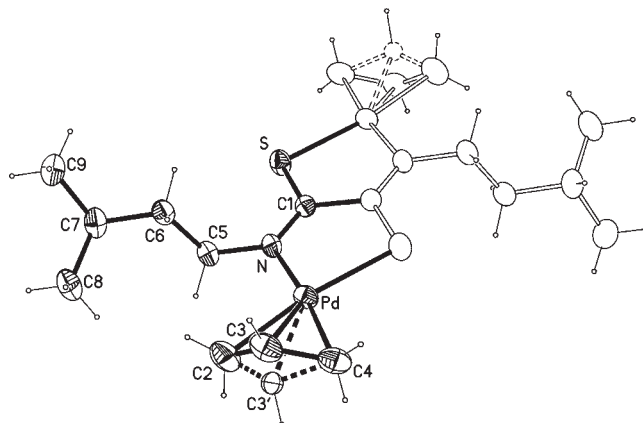
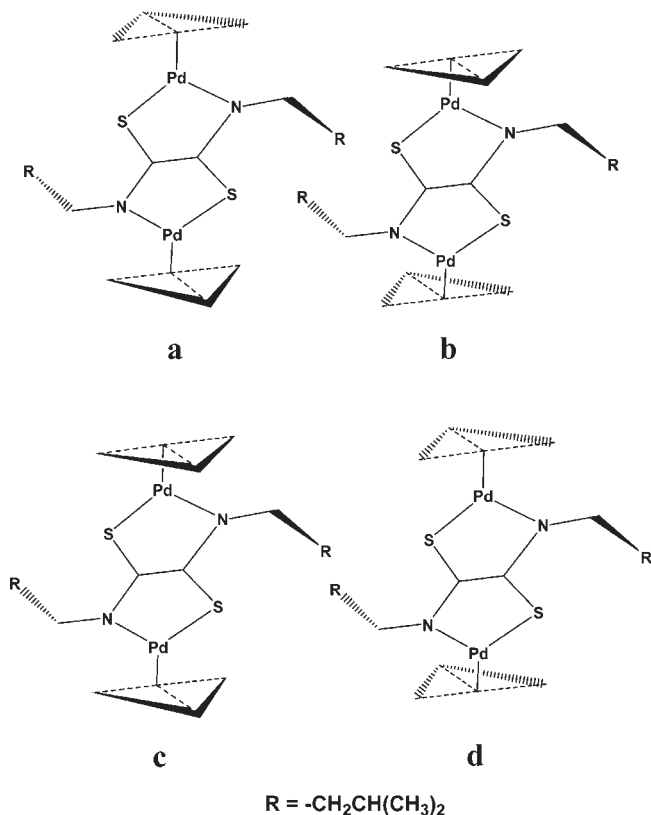


Figure 6. Perspective view of compound **5** showing its asymmetric unit (filled drawings) with the numbering scheme and its centrosymmetric equivalent (empty drawings). The two disordered allyl positions are represented by solid (85% of occupancy) and dotted (15%) lines, respectively. Thermal ellipsoids are drawn at the 30% probability level, while the hydrogen size is arbitrary.

Solid-State Structures. $[(\eta^3\text{-Allyl})\text{Pd}]_2(\mu\text{-isoamyl-DTO } \kappa\text{-N,S Pd}, \kappa\text{-N}',\text{S}' \text{ Pd}')$ (**5**). In the solid state, compound **5** is placed in a crystallographic center of symmetry that is right in the middle point of the central C–C bond of the DTO in a planar-transoid conformation (Figure 6). The molecular unit is centrosymmetric and is made up of equivalent halves. The isoamyl groups show a fixed conformation in the crystal packing. The terminal CH_2 carbon atoms of the allyl groups lie in the palladium coordination plane, while the central CH atom is split on opposite points with respect to the coordination plane. The central allyl CH disorder in η^3 -allylpalladium complexes is usually interpreted as the result of overlap of two conformations having a different position of the central CH, although several authors have interpreted such a disorder to be the result of thermal motion of the central allyl CH group.⁴⁵ In the crystal packing of compound **5**, the occupancy of the allyl cuspid oriented in the same direction of the nearest isoamyl group is 0.85, while it is 0.15 when the allyl CH is oriented in the opposite direction. This observed distribution ratio of the allyl orientation can be interpreted in two ways. First, we could presume that only the exo isomer exists (0.15, a; 0.85, b; 0, c; 0, d; Scheme 3) in the solid state because both conformers exhibit a centrosymmetrical arrangement. Second, the occupancy of the allyl cuspid oriented on the same side of the isoamyl group could also be 0.15 based on the distribution $0.075a + \frac{1}{2}(0.075c) + \frac{1}{2}(0.075d)$ (Chart 8) For the remaining 0.85, the occupancy could be due to the distribution $0.775b + \frac{1}{2}(0.075c) + \frac{1}{2}(0.075d)$ (Chart 8). Thus, the latter interpretation is

Chart 8. Orientation of Allyl Cuspids with Respect to the Nearest Isoamyl Group Observed in the Solid State for Complex 5 (See the Text)



compatible with the existence of 15% of the endo isomer in the crystal packing. This fact does not conflict with the observed symmetry of the crystal because species c and d, when equimolar, are a centrosymmetric racemate.

$[(\eta^3\text{-Allyl})\text{Pd}]_2[\mu\text{-}(\text{meso-DTO})\kappa\text{-}N,S\text{Pd},\kappa\text{-}N',S'\text{Pd}']$ (**7**). The unit cell **7** lies in a crystallographic center of symmetry, in the middle point of the C–C axis (Figure 7). The centrosymmetric molecule is made up of equivalent halves. In the solid state, the chiral alkyl groups show a fixed conformation. The CH₂ terminal carbon atoms of the allyl groups lie in the palladium coordination planes, while both allyl CH groups are split into two opposite positions with respect to the said molecular planes. In the crystal packing of **7**, the occupancy of allyl cuspids oriented in the same direction of the phenyl ring of the nearest (1-phenyl)ethyl substituent is 0.55, while it is 0.45 when the allyl CH group is oriented in the opposite direction. The observed distribution ratio may again be explained in two different ways. First, we could consider that the two pseudochiral exo isomers are the only species present in the solid state (0.45, a; 0.55, b; 0, c; 0, d; Chart 9) because both a and b meso forms exhibit a centrosymmetric arrangement. However, the occupancy of the allyl cuspid oriented on the same side of the phenyl group could also be 0.55 based on the distribution $0.225a, \frac{1}{2}(0.225c) + \frac{1}{2}(0.225d)$ (Chart 9). For the remaining 0.55, the occupancy is due to the following distribution $0.55b + \frac{1}{2}(0.225c) + \frac{1}{2}(0.225d)$. The presence of c and d (endo isomer) in the solid state is in agreement with the observed crystallographic symmetry, in that an equimolar mixture of c and d constitutes a

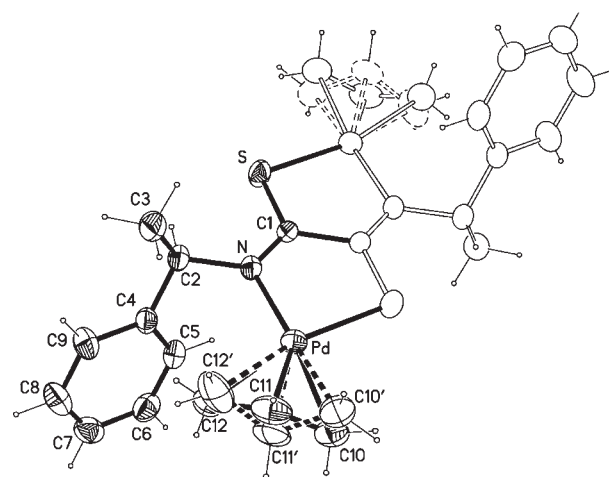
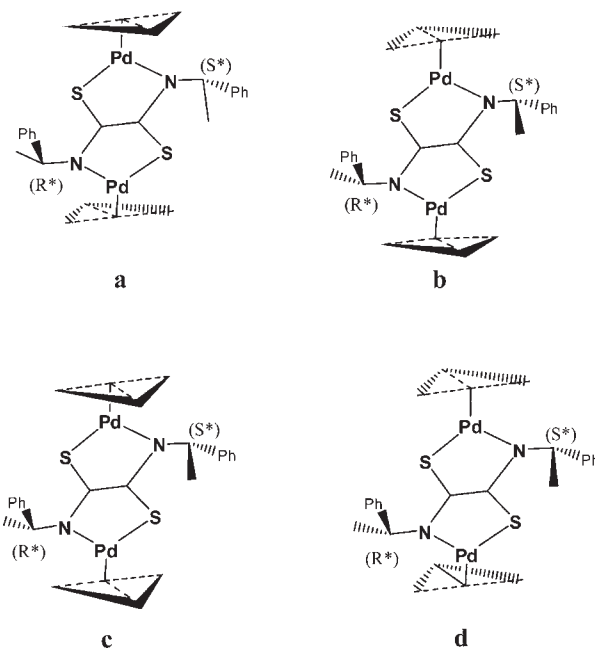


Figure 7. Perspective view of compound **7** constituted by the asymmetric unit (filled drawings) showing the numbering scheme and the centrosymmetric half part (empty drawings). The position of the disordered allyl with largest occupancy (55%) is denoted by solid lines and the other one (45%) by dotted lines. Thermal ellipsoids are drawn at the 30% probability level, while the hydrogen size is arbitrary.

Chart 9. Orientation of Allyl Cuspids with Respect to the Nearest Phenylethyl Group Observed in the Solid State for Complex 7 (See the Text)



centrosymmetric racemate. We would point out that the latter distribution is very similar to the isomeric composition observed in solution.

$[(\eta^3\text{-Allyl})\text{Pd}]_2[\mu\text{-}(\text{rac-DTO})\kappa\text{-}S,S'\text{Pd},\kappa\text{-}N,N'\text{Pd}']$ (**15**). In the solid state, **15** lies on a crystallographic 2-fold axis passing through the two palladium atoms (Figure 8). The crystal packing is centrosymmetric because it is constituted by equimolar quantities of chiral bimetallic molecules having opposite configuration, i.e., $[(\eta^3\text{-allyl})\text{Pd}]_2[\mu\text{-}[1\text{-}(S)\text{-}(1\text{-phenylethyl})]_2\text{-DTO}$

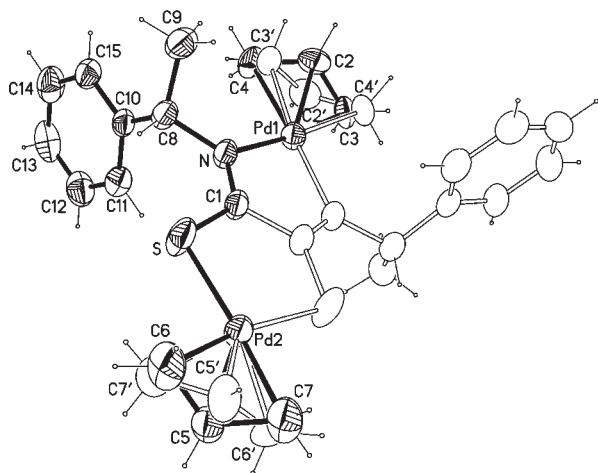


Figure 8. View of compound **15** evidencing the 2-fold axes passing through the palladium atoms and showing the numbering scheme of the asymmetric unit denoted by filled drawings. Each allyl ligand is split into two positions with equal occupancy (50%) as a consequence of symmetry. Thermal ellipsoids are drawn at the 30% probability level, while the hydrogen size is arbitrary.

$\kappa\text{-N,N}'\text{Pd}, \kappa\text{-S,S}'\text{Pd}'$] and $[(\eta^3\text{-allyl})\text{Pd}]_2[\mu\text{-}[1\text{-}(R)\text{-}(1\text{-phenylethyl})_2\text{-DTO } \kappa\text{-N,N}'\text{Pd}, \kappa\text{-S,S}'\text{Pd}']$. Each enantiomer is C_2 -symmetrical, and this implies that the occupancies of the two positions of the disordered allyl groups are equal (0.5). Crystal data of **15** agree with ^1H NMR spectra, which show equimolar mixtures of endo and exo isomers in solution.

CONCLUSION

In this paper, we have reported the synthesis and study of some homobimetallic complexes having two allylpalladium moieties joined by a binucleating DTO in both $\kappa\text{-N,N}'\text{Pd}, \kappa\text{-N}',\text{S}'\text{Pd}'$ and $\kappa\text{-N,N}'\text{Pd}, \kappa\text{-S,S}'\text{Pd}'$ coordination modes.

These linkage isomers show apparent allyl rotation: either in the $(\eta^3\text{-allyl})\text{Pd}(\text{N}^{\wedge}\text{N})$ — frame of $\kappa\text{-N,N}'\text{Pd}, \kappa\text{-S,S}'\text{Pd}'$ species or in both $(\eta^3\text{-allyl})\text{Pd}(\text{N}^{\wedge}\text{S})$ — frames of $\kappa\text{-N,N,S}\text{Pd}, \kappa\text{-N}',\text{S}'\text{Pd}'$ compounds. In the latter, the alkyldithiooxamidate group is therefore a double-hybrid hemilabile binucleating ligand. This implies that the use of DTO- containing chiral alkyl substituents as binucleating hybrid ligands could pave the way for studies on their role in hemilabile systems, which could easily carry and transfer chiral information.

$\kappa\text{-N,N}'\text{Pd}, \kappa\text{-S,S}'\text{Pd}'$ complexes in solution slowly change into the corresponding $\kappa\text{-N,N,S}\text{Pd}, \kappa\text{-N}',\text{S}'\text{Pd}'$ isomers presumably after breaking of the Pd—S bond in the $(\eta^3\text{-allyl})\text{Pd}(\text{S}^{\wedge}\text{S})$ — frame.

In other words, in $\kappa\text{-N,N}'\text{Pd}, \kappa\text{-S,S}'\text{Pd}'$ complexes, Pd—N bond rupture produces stereoisomerization (allyl pseudorotation) at the NMR time scale, while Pd—S bond breaking causes linkage isomerization over a much longer time scale. It would therefore be interesting to explore the possible catalytic activity in bimetallic systems where each of the two metals can produce a vacant coordination site under different energetic conditions.

AUTHOR INFORMATION

Corresponding Author

*E-mail: lanza@unime.it.

REFERENCES

- (1) Lanza, S.; Bruno, G.; Nicolò, F.; Scopelliti, R. *Tetrahedron: Asymmetry* **1996**, *7*, 3347–3350.
- (2) Lanza, S.; Bruno, G.; Nicolò, F.; Rotondo, A.; Scopelliti, R.; Rotondo, E. *Organometallics* **2000**, *19* (13), 2462–2469.
- (3) Lanza, S.; Bruno, G.; Nicolò, F.; Callipari, G.; Tresoldi, G. *Inorg. Chem.* **2003**, *42*, 4545–4552.
- (4) Lanza, S.; Callipari, G.; Loiseau, F.; Serroni, S.; Tresoldi, G. *Inorg. Chem.* **2005**, *44*, 6717–6724.
- (5) Veit, R.; Girerd, J. J.; Kahn, O.; Jeannin, Y.; Robert, F.; El Murr, N. *Inorg. Chem.* **1984**, *23*, 4448–4454.
- (6) Ye, Q. Y.; Nakaro, Y.; Frauenhoff, G. R.; Whitcomb, D. R.; Takusagava, F.; Busch, D. H. *Inorg. Chem.* **1991**, *30*, 1503–1510.
- (7) Girerd, J. J.; Jeannin, S.; Jeannin, Y.; Kahn, O. *Inorg. Chem.* **1978**, *17*, 3034–3040.
- (8) Cotton, F. A.; Li, Z.; Liu, C. Y.; Murillo, C. A. *Inorg. Chem.* **2007**, *46*, 7840–7847.
- (9) Lanza, S.; Bruno, G.; Nicolò, F.; Rotondo, A.; Tresoldi, G. *Eur. J. Inorg. Chem.* **2002**, 65–72.
- (10) Lanza, S.; Giannetto, A.; Bruno, G.; Nicolò, F.; Tresoldi, G. *Eur. J. Inorg. Chem.* **2009**, 2647–2654.
- (11) Lanza, S.; Nicolò, F.; Cafeo, G.; Amiri Rudbari, H.; Bruno, G. *Inorg. Chem.* **2010**, *49*, 9236–9246.
- (12) Hurd, R. N.; De La Mater, G.; McElheny, C. G.; Turner, R. J.; Vallingford, V. H. *J. Org. Chem.* **1961**, *26*, 3980–3987.
- (13) (a) COSMO, version 1.60; Bruker AXS Inc.: Madison, WI, 2005. (b) SAINT, version 7.06A; Bruker AXS Inc.: Madison, WI, 2005. (c) SADABS, version 2.10; Bruker AXS Inc.: Madison, WI, 2005.
- (14) SIR2004; Burla, M. C.; Caliendo, R.; Camalli, M.; Carrozzini, B.; Cascarano, G. L.; De Caro, L.; Giacovazzo, C.; Polidori, G.; Spagna, R. *J. Appl. Crystallogr.* **2005**, *38*, 381–388.
- (15) Sheldrick, G. M. *SHELXL97*; University of Göttingen: Göttingen, Germany, 1997.
- (16) Frisch, M. J.; Trucks, G. W.; Schlegel, H. B.; Scuseria, G. E.; Robb, M. A.; Cheeseman, J. R.; Montgomery, J. A.; Vreven, T.; Kudin, K. N.; Burant, J. C.; Millam, J. M.; Iyengar, S. S.; Tomasi, J.; Barone, V.; Mennucci, B.; Cossi, M.; Scalmani, G.; Rega, N.; Petersson, G. A.; Nakatsuji, H.; Hada, M.; Ehara, M.; Toyota, K.; Fukuda, R.; Hasegawa, J.; Ishida, M.; Nakajima, T.; Honda, Y.; Kitao, O.; Nakai, H.; Klene, M.; Li, X.; Knox, J. E.; Hratchian, H. P.; Cross, J. B.; Adamo, C.; Jaramillo, J.; Gomperts, R.; Stratmann, R. E.; Yazyev, O.; Austin, A. J.; Cammi, R.; Pomelli, C.; Ochterski, J. W.; Ayala, P. Y.; Morokuma, K.; Voth, G. A.; Salvador, P.; Dannenberg, J. J.; Zakrzewski, V. G.; Dapprich, S.; Daniels, A. D.; Strain, M. C.; Farkas, O.; Malick, D. K.; Rabuck, A. D.; Raghavachari, K.; Foresman, J. B.; Ortiz, J. V.; Cui, Q.; Baboul, A. G.; Clifford, S.; Cioslowski, J.; Stefanov, B. B.; Liu, G.; Liashenko, A.; Piskorz, P.; Komaromi, I.; Martin, R. L.; Fox, D. J.; Keith, T.; Al-Laham, M. A.; Peng, C. Y.; Nanayakkara, A.; Challacombe, M.; Gill, P. M. W.; Johnson, B.; Chen, W.; Wong, M. W.; Gonzalez, C.; Pople, J. A. *Gaussian 03*, revision B.04; Gaussian, Inc.: Pittsburgh, PA, 2003.
- (17) Adamo, C.; Barone, V. *J. Chem. Phys.* **1999**, *110*, 6158–6170.
- (18) Ernzerhof, M.; Scuseria, G. E. *J. Chem. Phys.* **1999**, *110*, 5029–5036.
- (19) (a) Figgen, D.; Rauhut, G.; Dolg, M.; Stoll, H. *Chem. Phys.* **2005**, *311*, 227–244. (b) Peterson, K. A.; Puzzarini, C. *Theor. Chem. Acc.* **2005**, *114*, 283–296.
- (20) (a) Faller, J. W.; Sarantopoulos, N. *Organometallics* **2004**, *23*, 2008–2014. (b) Faller, J. W.; Stokes-Huby, H. L.; Albrizzio, M. A. *Helv. Chim. Acta* **2001**, *84*, 3031–3042.
- (21) (a) Gómez-de la Torre, F.; de la Hoz, A.; Jalón, F. A.; Manzano, B. R.; Rodríguez, A. M.; Elguero, J.; Martínez-Ripoll, M. *Inorg. Chem.* **2000**, *39*, 1152–1162. (b) Gómez-de la Torre, F.; de la Hoz, A.; Jalón, F. A.; Manzano, B. R.; Otero, A.; Rodríguez, A. M.; Rodríguez-Perez, M. C.; Aurea Echevarría, P.; Elguero, J. *Inorg. Chem.* **1998**, *37*, 6606–6614. (c) Berenguer, J. R.; Forniés, J.; Lalinde, E.; Martínez, F. *Organometallics* **1996**, *15*, 4537–4546. (d) Tsukada, N.; Sato, T.; Mori, H.; Sugawara, S.; Kabuto, C.; Miyano, S.; Inoue, Y. *J. Organomet. Chem.* **2001**, *627*, 121–126. (e) Scrivanti, A.; Benetollo, F.; Venzo, A.

Bertoldini, M.; Beghetto, V.; Matteoli, U. *J. Organomet. Chem.* **2007**, *692*, 3577–3582.

(22) (a) Prelog, V. *Proc. K. Ned. Akad. Wet., Ser. B: Phys. Sci.* **1968**, *B71*, 108–123. (b) Prelog, V. *Problems in chemical topology. Twenty-first organic chemistry Symposium of American Chemical Society*; American Chemical Society: Columbus, OH, 1969; pp 72–84.

(23) Helmchen, G. *Recent Developments in the Relations between Geometry and Stereochemistry; Lecture presented at the Annual Chemical Congress of the Chemical Society*; Royal Society of Chemistry: London, Mar 30, 1977.

(24) (a) Goldberg, S. I.; Baileyl, W. D. *J. Am. Chem. Soc.* **1971**, *93*, 1046–1047. (b) Goldberg, S. I.; Baileyl, W. D. *J. Am. Chem. Soc.* **1974**, *96*, 6381–6387.

(25) Ganter, C.; Brassat, L.; Glinsböckel, C.; Ganter, B. *Organometallics* **1997**, *16*, 2862–2867.

(26) Braunstein, P.; Naud, F. *Angew. Chem., Int. Ed.* **2001**, *40*, 680–699.

(27) Braunstein, P. *J. Organomet. Chem.* **2004**, *689*, 3953–3967.

(28) Jeffrey, J. C.; Rauchfuss, T. B. *Inorg. Chem.* **1979**, *18*, 2658–2666.

(29) (a) Braunstein, P.; Matt, D.; Mathey, F.; Thavard, D. *J. Chem. Res.* **1978**, 232, 3041. (b) Braunstein, P.; Matt, D.; Dusausoy, Y.; Fischer, J.; Mitschler, A.; Ricard, L. *J. Am. Chem. Soc.* **1981**, *103*, 5115–5125. (c) Braunstein, P.; Matt, D.; Dusausoy, Y. *Inorg. Chem.* **1983**, *22*, 2043–2047. (d) Braunstein, P.; Fischer, J.; Matt, D.; Pfeffer, M. *J. Am. Chem. Soc.* **1984**, *106*, 410–421.

(30) (a) Braunstein, P.; Naud, F.; Dedieu, A.; Rohmer, M. M.; DeCian, A.; Rettig, S. *Organometallics* **2001**, *20*, 2966–2981. (b) Braunstein, P.; Zhang, J.; Welter, R. *Dalton Trans.* **2003**, 507–509.

(31) Ankersmit, H. A.; Loken, B. H.; Kooijman, H.; Spek, A. L.; Vrieze, K.; van Koten, G. *Inorg. Chim. Acta* **1996**, *252*, 141–155.

(32) Fernández-Galán, R.; Jalón, F. A.; Manzano, B. R.; Rodríguez-de la Fuente, J.; Vrahami, M.; Jedlicka, B.; Weissensteiner, W.; Jogl, G. *Organometallics* **1997**, *16*, 3758–3768.

(33) Scheele, U. J.; John, M.; Dechert, S.; Meyer, F. *Eur. J. Inorg. Chem.* **2008**, 373–377.

(34) (a) Faller, J. W.; Wilt, J. C. *Organometallics* **2005**, *24*, 5076–5083. (b) Faller, J. W.; Milheiro, S.; Parr, J. J. *Organomet. Chem.* **2008**, *693*, 1478–1493. (c) Milheiro, S. C.; Faller, J. W. *J. Organomet. Chem.* **2011**, *696*, 879–886.

(35) Brassat, J.; Englert, U.; Keim, W.; Keitel, D. P.; Killat, S.; Suranna, J. P.; Wang, R. *Inorg. Chim. Acta* **1998**, *280*, 150–162.

(36) (a) Canovese, L.; Visentin, F.; Uguagliati, P.; Chessa, G.; Pesce, A. *J. Organomet. Chem.* **1998**, *566*, 61–71. (b) Canovese, L.; Visentin, F.; Uguagliati, P.; Lucchini, V.; Bandoli, G.; Chessa, G. *Inorg. Chim. Acta* **1998**, *275–276*, 385–394.

(37) Yang, H.; Khan, M. A.; Nicholas, K. M. *Organometallics* **1993**, *12*, 3485–3494.

(38) Variable-temperature (VT) experiments have not been performed in the complexes bearing chiral amine-derived ligands because allyl signals of various diastereomers could have not collapsed because of the presence of chiral centers in the molecular plane. Only NCH-(CH₃)C₆H₅ doublets could collapse because in these complexes they are correlated by a symmetry operation. However, these doublets are so close to each other that the results of the rate measurement would be of marginal significance. Rates and activation parameters are inaccessible also for kinetic complexes (κ -N,N' Pd, κ -S,S' Pd') bearing achiral amine-derived ligands. In these complexes, the allyl group in the (η^3 -allyl)Pd-(S^ \wedge S)- frame does not isomerize; thus, the molecular plane cannot become symmetrical. As a consequence, NCH₂ protons cannot become equivalent. Furthermore, VT experiments performed on κ -N,N' Pd, κ -S, S' Pd' complexes could be affected also by the change of these species into the N,S Pd, κ -N',S' Pd' compounds. Thus, only in the thermodynamic complexes (κ -N,S Pd, κ -N',S' Pd') could the ABX_n signals of NCH₂ groups become a more simple A₂X_n spin system without other complications. Actually, we tried to perform VT experiments on these latter complexes. Unfortunately, we obtained very poor results: in deuterated tetrachloroethane at about 80 °C, the ABX_n signals were still far from collapsing to the A₂X_n spectral pattern.

(39) (a) Albinati, A.; Amman, C. J.; Pregosin, P. S.; Ruegger, P. S. *Organometallics* **1990**, *9*, 1826–1833. (b) Albinati, A.; Kunz, R. W.; Amman, C. J.; Pregosin, P. S. *Organometallics* **1991**, *10*, 1800–1806.

(40) Pearson, R. G. *J. Am. Chem. Soc.* **1963**, *85*, 3533–3539.

(41) (a) Pearson, R. G. *Acc. Chem. Res.* **1993**, *26*, 250–255. (b) Pearson, R. G. *J. Chem. Educ.* **1999**, *76*, 267–275.

(42) Del Campo, O.; Carbayo, A.; Cuevas, J. V.; García-Erbosa, G.; Muñoz, A. *Eur. J. Inorg. Chem.* **2009**, *15*, 2254–2260.

(43) Fave, C.; Hissler, M.; Sénéchal, K.; Ledoux, I.; Zyss, J.; Réau, R. *Chem. Commun.* **2002**, *16*, 1674–1675.

(44) Angurell, I.; Ferrer, M.; Gutiérrez, A.; Martínez, M.; Rodríguez, L.; Rossel, O.; Engeser, M. *Chem.—Eur. J.* **2010**, *16*, 13960–13964.

(45) Redon, R.; Torrens, H.; Ekkehardt Hahn, F.; Lügger, T.; Hernandez-Ortega, S.; Toscano, R. A.; Morales-Morales, D. *J. Mol. Struct.* **2003**, *655*, 423–433.